Discretization of a new model of dispersive waves with improved dispersive properties and exact conservation of energy

Arnaud Duran, Gaël Loïc Richard

Discretization of a new model of dispersive waves with improved dispersive properties and exact conservation of energy

Arnaud Duran[1,2] and Gaël L. Richard[3]

[1] Institut Camille Jordan, Université Claude Bernard Lyon 1. *arnaud.duran@univ-lyon1.fr.*
[2] Institut Universitaire de France.
[3] Univ. Grenoble Alpes, INRAE, IGE, Grenoble, France. *gael.richard@inrae.fr*

Abstract

In this work, we derive a hyperbolic system of dispersive equations for the numerical simulation of coastal waves with improved dispersive properties and admitting an exact energy conservation equation. This system is derived with the assumption of a moderate non-linearity and of a correction coefficient close to 1. This system contains the same non-linear terms as the Serre-Green-Naghdi equations, which are obtained in the limit where the Mach number tends to zero. The assumptions are only used to neglect non-linear terms related to the improvement of dispersive properties. The bathymetry can be included with a mild-slope hypothesis. On this basis, we propose an energy-stable numerical scheme relying on a splitting between the hyperbolic and dispersive parts of the model. The stability of the method is achieved through the discrete dissipation of the energy balance specific to each step. We also establish the existence of soliton solutions for this model. Numerical simulations are proposed to highlight the dispersive properties of the model, as well as the dissipative character of the scheme.

Introduction

In view of the increasing frequency and intensity of extreme events such as tsunamis and major storms, it is of fundamental importance to have a rapid and reliable description of water wave models. Despite constant progress in terms of computing and parallel calculation, the free surface Euler equations - that integrate the complete 3d velocity field - are still out of reach from an operational point of view. This is where simplified models of shallow water type come into play, exploiting the low relative variability of the flow along the vertical coordinate to reduce the dimensionality of the problem. One of the most classic models is the so-called Non-Linear Shallow Water (NLSW) model, which is effective in capturing the main non-linear dynamics in the surf zone. This model is also relevant to describe breaking waves thanks to its hyperbolic structure, seeing breaking waves as shocks, as well as run-up and run-down mechanisms during flooding and submersion events. Nevertheless, it proves ineffective in deeper waters, as it neglects the phenomenon of dispersion, which is predominant before the breaking point, in the shoaling zone. The first model capable of taking these effects into account was proposed by Boussinesq in

[5], and extended by Peregrine [49] in the presence of a variable bottom. Boussinesq-type models have since taken a central role in water wave modelling. Removing the scaling assumption on the relative amplitude of the wave, fully nonlinear equations were proposed by Serre [55], and extended to 2D by Green & Naghdi [27]. These equations will be referred to as SGN equations in the following. This class of models can be derived as approximations of the free-surface Euler equations in the shallow-water regime (see [33] for a rigorous justification), in an asymptotic of higher order than the NLSW equations.

In a more recent period, for around thirty years, Boussinesq-type models were subject to numerous improvements to extend their validity domain, in particular regarding linear dispersion characteristics. One of the first works was proposed by Madsen & Sorensen [39] in the weakly non-linear case, with the derivation of an augmented model implying higher-order terms, allowing to reach a better dispersion relation. Nwogu [46] also proposed extended equations relying on a new variable corresponding to the velocity at a certain depth, still in the Boussinesq regime. This approach was shortly afterwards extended to the fully non-linear case in [58]. These first works paved the way for a series of successive improvements, most of them eventually resulting in free-parameter models enabling an appropriate adjustement of the linear frequency dispersion. We refer for instance to [3], [4], [7], [35], [40], [41] for a non exhaustive list. More recently, interest has also focused on multi-layer approaches, allowing a natural improvement of linear dispersion characteristics (see for instance [22], [26], [36]). Generally speaking, some of these strategies can change the structure of the equations (mainly due to the presence of additional equations or/and higher order derivatives), which makes them more costly and more technical to implement numerically, with the added threat of impacting the well-posed character of the problem. On the other hand, some free-parameter methods only imply minor modifications of the original model, but at the price of compromising the exact preservation of the energy balance (see for instance [4], [7]). In this context, one of the few attempts to reconcile improved dispersive properties and an exact energy equation has been proposed in [9]. The method relies on a modified Lagrangian formulation of the Serre equations, allowing to introduce a free parameter to enhance dipersion relation without breaking the energy balance. Also, from a more general point of view, although they are outside the scope of the present study, some results of this nature are available within the frame of formulations in terms of velocity potential; one may refer to [15], [19] for instance for full dispersion models implying Fourier multipliers.

As regards numerical discretization, there is now a wide variety of approaches available in the literature dedicated to the SGN equations, mainly based on usual methods such as Finite Volumes (FV), Finite Differences (FD), continuous Finite Elements (FEM), discontinuous Galerkin (dG), or hybrid methods. For a non exhaustive list of examples in 1d, one may refer to [8], [43] (hybrid FV/FD), [13], [47],[59] (dG), [44] (FEM), or also [50] for a FV approach for the model [9]. Recently, one strategy entering the formalism of hybrid methods is to exploit the projection structure of the SGN equations, interpreting the system as a hyperbolic problem with constraint (see the recent references [26], [45]). The list of work carried out in 2d is more limited. On cartesian grids, one may refer to the hybrid FV/FD methods employed in [4], [34], [51], [57], and the dG methods developed in [37], [54] for instance. On unstructured meshes, the dG schemes [16], [42], and the hybrid FV/FEM method [31] are one of the few numerical models available. However,

these approaches based on the original formulation of the SGN equations have in common the need to invert a time-dependent elliptic operator, which constitutes a major technical obstacle for operational applications. Although strategies have recently been proposed to relax the computation time and facilitate implementation issues ([28], [34]), these direct approaches remain generally very costly, cumbersome to set up and limit the possibilities of parallelization, especially on general meshes.

Due to these limitations, a recent trend is to use hyperbolisation techniques to provide approximate versions of the SGN equations, with a structure more favourable in view of numerical implementation. A first proposition in that direction has been made in [23], and recently extended in 2D on cartesian grids [56]. The principle is to return to the Lagrangian formulation of the SGN equations and modify it in order to recover a first-order model which tends formally towards SGN in the limit of a relaxation parameter (this limit has been rigorously justified in [14]). This results in a hyperbolic model with source term, naturally admitting an energy balance. Another hyperbolization technique has been proposed in [20], work in which authors introduce artificial compressibility to obtain the relaxation limit. This work has been extended shortly after in [21] to cover a more general class of Boussinesq-type models. In the same spirit, another extension has been proposed in [52], where the model is directly derived from the free surface Euler equations under a weakly compressibility assumption. This method allows to recover the one derived in [20] in the incompressible limit, and dispersive properties are improved introducing a free parameter in the model, in the same spirit than [4]. Here again, this improvement is achieved at the cost of breaking the exact energy equation, which is only asymptotically satisfied. The numerical resolution for [23], [56] relies on an operator splitting based on a standard Finite Volume approach for the hyperbolic part and an exact resolution of an ODE for the relaxation part. More recently, important efforts have been made regarding the development of efficient algorithms for these models. Numerical schemes of type ADER-DG have been proposed in 2d on structured grids in [20] and [6]; these algorithms are supplemented by an *a posteriori* limiting procedure of MOOD type to guarantee stability. At the same time, FEM were used in [24] and [25] for an extension of the model [23] including all the bathymetry terms; in these works, numerical stability issues are addressed through positivity and well-balancing properties, and rely on the choice of appropriate viscosity terms.

However, in all the above-mentioned works, whether for the SGN equations or their current hyperbolic approximations, it appears that the problem of energy conservation at the discrete level has not been thoroughly examined. As regards the SGN system, results can be found in [45], where the discrete energy stability is directly inherited from the native features of the projection method. Concerning hyperbolic models approximating the SGN equations, up to the authors knowledge, the only scheme offering such guarantees at the fully discrete level is the splitting strategy proposed in [23] in 1d and on a flat bottom. In the light of the issues raised above, the aim of the proposed work is twofold:

- In the weakly compressible case, extend the model [52] (see also [20]) in order to improve its dispersive properties, while maintaining an exact energy balance.
- Propose a numerical scheme capable of preserving this energy balance in a fully discrete framework.

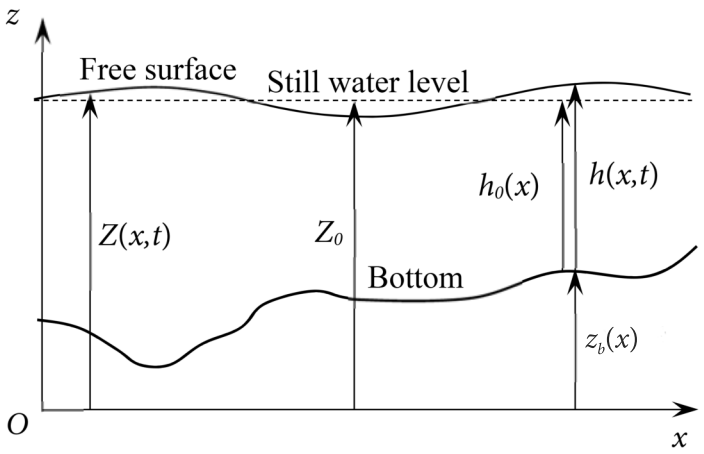

Figure 1: Definition sketch.

This paper presents first results obtained in the 1d case and under a hypothesis of mild slope. It is structured as follows: in Section §1 we focus on the derivation of the model with improved dispersive properties and an exact energy equation. We study its characteristics and show the existence of exact soliton solutions. Then, the Section §2 presents the proposed scheme and the main results related to its stability. The Section §3 proposes a series of test cases attesting to the enhancement of the linear frequency dispersion relation and the dissipative character of the scheme. The technical details related to the derivation of the soliton solution and the proofs of the lemmas necessary for the stability of the scheme are available in Section §4.

1 Model derivation and properties

1.1 Derivation of the model with improved dispersive properties and exact energy conservation

We study a flow of depth h over a bathymetry determined by the bottom elevation z_b measured from an arbitrary horizontal datum (see Figure 1). The free surface elevation is denoted by Z if it is measured from this horizontal datum and is denoted by η if it is measured from the still water level. Note that Z and η differs by a constant Z_0, which is the still water level measured from the horizontal datum. The still water depth is h_0. We have thus $Z = Z_0 + \eta = z_b + h = z_b + h_0 + \eta$. Denoting by L a characteristic length for the variations of the flow in the horizontal direction and by H a characteristic depth, the shallow-water approximation is assumed to be valid. The parameter

$$\varepsilon = \frac{H}{L} \ll 1 \tag{1}$$

is thus a small parameter. The characteristic wave amplitude of the free surface elevation measured from the still water level is denoted by A. We assume a moderate non-linearity,

which means that the non-linearity parameter δ is of $O(\varepsilon)$, i.e.

$$\delta = \frac{A}{H} = \varepsilon. \tag{2}$$

This implies that

$$\frac{\partial \eta}{\partial x} = O(\varepsilon^2). \tag{3}$$

A characteristic fluid velocity in the horizontal direction is denoted by u_0. The Froude number F is also supposed to be small and of the same order of magnitude as the non-linearity parameter, which implies

$$F = \frac{u_0}{\sqrt{gH}} = \delta = \varepsilon. \tag{4}$$

We start from the hyperbolic system with improved dispersive properties derived in Richard (2021) [52] where U is the depth-averaged fluid velocity and W is the vertical fluid velocity at a relative height $\alpha/2$ above the bottom with respect to the water depth. We can thus define

$$\frac{\alpha}{2} = \frac{z - z_b}{h}. \tag{5}$$

The coefficient α is larger than 1 and coincides with the coefficient of the method of Bonneton *et al.* (2011) [4]. The model [52] has several variants. Since the goal of the present work is to model coastal waves, where compressible effects are negligible, and not tsunamis in deep oceans, we use the quasi-incompressible set of equations where the static compressibility is neglected. Moreover, we use a mild-slope assumption, which, in the case of a moderate nonlinearity, means that

$$\frac{\partial z_b}{\partial x} = O(\varepsilon^4). \tag{6}$$

With these conditions and assumptions, the system obtained in [52] includes five equations. The first three equations are a mass conservation equation

$$\frac{\partial \tilde{h}}{\partial \tilde{t}} + \varepsilon \frac{\partial \tilde{h}\tilde{U}}{\partial \tilde{x}} = 0\,, \tag{7}$$

a momentum balance equation in the horizontal direction

$$\frac{\partial \tilde{h}\tilde{U}}{\partial \tilde{t}} + \frac{\partial}{\partial \tilde{x}}\left(\varepsilon \tilde{h}\tilde{U}^2 + \frac{\tilde{h}^2}{2} + \varepsilon^2 \tilde{h}\tilde{P}\right) = -\varepsilon^2 \tilde{h}\frac{\partial \tilde{z}_b}{\partial \tilde{x}} + O(\varepsilon^4), \tag{8}$$

and a momentum balance equation in the vertical direction

$$\frac{\partial \tilde{h}\tilde{W}}{\partial \tilde{t}} + \varepsilon \frac{\partial \tilde{h}\tilde{U}\tilde{W}}{\partial \tilde{x}} = \frac{3}{2}\tilde{P} + \frac{\alpha - 1}{2\alpha}\tilde{h}^2 \frac{\partial \tilde{S}}{\partial \tilde{x}} + 4\varepsilon \frac{\alpha - 1}{\alpha^2}\tilde{W}^2 + O(\varepsilon^3). \tag{9}$$

These equations are written in dimensionless form (a tilde denotes a dimensionless quantity). In these equations, P is the depth-averaged non-hydrostatic pressure and S is a variable proportional to the free surface slope defined by

$$S = \alpha \frac{\partial Z}{\partial x} = \alpha \frac{\partial \eta}{\partial x}. \tag{10}$$

The dimensionless quantities are defined as follows

$$\begin{aligned} &\tilde{U} = \frac{U}{u_0} = \frac{U}{\varepsilon\sqrt{gH}}\,; \quad \tilde{h} = \frac{h}{H}\,; \quad \tilde{W} = \frac{W}{\varepsilon^2\sqrt{gH}}\,; \quad \tilde{P} = \frac{P}{\varepsilon^3 gH}\,; \\ &\tilde{t} = t\frac{\sqrt{gH}}{L}\,; \quad \tilde{x} = \frac{x}{L}\,; \quad \tilde{S} = \frac{S}{\varepsilon^2}\,; \quad \frac{\partial \tilde{z}_b}{\partial \tilde{x}} = \frac{1}{\varepsilon^4}\frac{\partial z_b}{\partial x}\,. \end{aligned} \tag{11}$$

The moderate nonlinearity assumption and the mild slope assumption lead to

$$\frac{\partial h}{\partial x} = \varepsilon^2\frac{\partial \tilde{\eta}}{\partial \tilde{x}} - \varepsilon^4\frac{\partial \tilde{z}_b}{\partial \tilde{x}}\,; \quad \frac{\partial \tilde{h}}{\partial \tilde{x}} = \varepsilon\frac{\partial \tilde{\eta}}{\partial \tilde{x}} - \varepsilon^3\frac{\partial \tilde{z}_b}{\partial \tilde{x}}. \tag{12}$$

The two last equations are firstly a relaxation equation for P, which is written

$$\frac{\partial \tilde{h}\tilde{P}}{\partial \tilde{t}} + \varepsilon\frac{\partial \tilde{h}\tilde{U}\tilde{P}}{\partial \tilde{x}} = -\frac{1}{M_0^2}\left(2\tilde{W} + \alpha\tilde{h}\frac{\partial \tilde{U}}{\partial \tilde{x}} + O(\varepsilon^2)\right) \tag{13}$$

and secondly an evolution equation for S, which is

$$\frac{\partial \tilde{h}\tilde{S}}{\partial \tilde{t}} + \varepsilon\frac{\partial \tilde{h}\tilde{U}\tilde{S}}{\partial \tilde{x}} = 2\tilde{h}\frac{\partial \tilde{W}}{\partial \tilde{x}} + \varepsilon\frac{2}{\alpha}\tilde{W}\tilde{S} + O(\varepsilon^3). \tag{14}$$

The dimensionless number M_0 is a Mach number defined as

$$M_0 = \frac{\sqrt{gH}}{a}\,, \tag{15}$$

where a is the sound velocity. M_0 is a very small parameter controlling the relaxation of the vertical velocity W. However, since the real compressibility is wholly negligible in the case of coastal waves, an artificial compressibility method can be used in order to obtain a hyperbolic system of equations, which means that the sound velocity can be artificially reduced. This implies that the left-hand side of (13) is only useful for obtaining a hyperbolic approximation to the model with improved dispersive properties of [4].

It should be noted that the variables W and S are only involved in (8) through the term $\varepsilon^2 hP$, which is $O(\varepsilon^2)$. Consequently, we can neglect in equations (9) and (14) the terms scaled as $O(\varepsilon^2)$, since they finally bring $O(\varepsilon^4)$ corrections. However, we keep the terms in $O(\varepsilon)$ in these equations which actually correspond to $O(\varepsilon^3)$ corrections. The model is thus consistent up to $O(\varepsilon^3)$ in (8) and up to $O(\varepsilon)$ in (9) and (14). This system is obtained assuming a decomposition of the fluid horizontal velocity of the form $u = U + \varepsilon^\beta u'$. The terms due to the deviation u' to the depth-averaged value of the velocity are of $O(\varepsilon^{2\beta+1})$ in (8) and of $O(\varepsilon^{1+\beta})$ in (9). We assume that the flow is irrotational, which implies that $\beta = 2$.

Because of the mild-slope assumption, the bathymetric terms are of $O(\varepsilon^4)$ in (8) and of $O(\varepsilon^3)$ in (9), (13) and (14), and are also negligible, except the term $-\varepsilon^2\tilde{h}\partial\tilde{z}_b/\partial\tilde{x}$ in (8). As for the system with improved dispersive properties of [4], the system of equations (7), (8), (9), (13) and (14) does not admit an exact equation of energy conservation. In order to obtain an exact conservation of energy, the system of equations has to be rewritten with an additional assumption. The correction coefficient α governs the improvement of dispersive properties, as in [4], [52]. The usual value is $\alpha = 1.159$ (see [4]). In the following, α is assumed to be close to 1. We thus define α' by

$$\alpha' = \alpha - 1\,, \tag{16}$$

which is scaled as

$$\tilde{\alpha}' = \frac{\alpha'}{\varepsilon} \tag{17}$$

where $\tilde{\alpha} = O(1)$. Therefore equation (9) can be written in dimensionless form

$$\frac{\tilde{h}\tilde{W}}{\partial \tilde{t}} + \varepsilon \frac{\partial \tilde{h}\tilde{U}\tilde{W}}{\partial \tilde{x}} = \frac{3}{2}\tilde{P} + \varepsilon \frac{\tilde{\alpha}'}{2\alpha}\tilde{h}^2 \frac{\partial \tilde{S}}{\partial \tilde{x}} + O(\varepsilon^2). \tag{18}$$

We define the quantity B as

$$B = S\sqrt{h} = \alpha\sqrt{h}\frac{\partial \eta}{\partial x}, \tag{19}$$

which is scaled as

$$\tilde{B} = \frac{B}{\varepsilon^2\sqrt{h_0}}. \tag{20}$$

Thanks to the assumption of a moderate nonlinearity, the derivative of $\tilde{S}$ can be written

$$\frac{\partial \tilde{S}}{\partial \tilde{x}} = \frac{1}{\sqrt{\tilde{h}}}\frac{\partial \tilde{B}}{\partial \tilde{x}} + O(\varepsilon). \tag{21}$$

Therefore, equation (18) can be rewritten, at the same approximation order:

$$\frac{\tilde{h}\tilde{W}}{\partial \tilde{t}} + \varepsilon \frac{\partial \tilde{h}\tilde{U}\tilde{W}}{\partial \tilde{x}} = \frac{3}{2}\tilde{P} + \varepsilon \frac{\tilde{\alpha}'}{2\alpha}\tilde{h}^{3/2} \frac{\partial \tilde{B}}{\partial \tilde{x}} + O(\varepsilon^2)\,. \tag{22}$$

Using the mass conservation equation, we obtain an evolution equation for the quantity B writing

$$\frac{\partial \tilde{h}\tilde{B}}{\partial \tilde{t}} + \varepsilon \frac{\partial \tilde{h}\tilde{U}\tilde{B}}{\partial \tilde{x}} = \tilde{h}\frac{\mathrm{D}\tilde{B}}{\mathrm{D}\tilde{t}}\,, \tag{23}$$

where the material derivative is defined by $\mathrm{D}/\mathrm{D}t = \partial/\partial t + U\partial/\partial x$. Replacing B using (19) yields

$$\tilde{h}\frac{\mathrm{D}\tilde{B}}{\mathrm{D}\tilde{t}} = \tilde{h}^{3/2}\frac{\mathrm{D}\tilde{S}}{\mathrm{D}\tilde{t}} + \varepsilon\frac{\sqrt{\tilde{h}}}{2}\tilde{S}\frac{\mathrm{D}\tilde{h}}{\mathrm{D}\tilde{t}}. \tag{24}$$

Using again the mass conservation, we can write the equality

$$\tilde{h}\frac{\mathrm{D}\tilde{S}}{\mathrm{D}\tilde{t}} = \frac{\partial \tilde{h}\tilde{S}}{\partial \tilde{t}} + \varepsilon\frac{\partial \tilde{h}\tilde{U}\tilde{S}}{\partial \tilde{x}}. \tag{25}$$

Equation (14) and the mass conservation (7) yield

$$\frac{\partial \tilde{h}\tilde{B}}{\partial \tilde{t}} + \varepsilon \frac{\partial \tilde{h}\tilde{U}\tilde{B}}{\partial \tilde{x}} = \sqrt{\tilde{h}}\left(2\tilde{h}\frac{\partial \tilde{W}}{\partial \tilde{x}} + \varepsilon\frac{2}{\alpha}\tilde{W}\tilde{S}\right) - \varepsilon\frac{h^{3/2}}{2}\tilde{S}\frac{\partial \tilde{U}}{\partial \tilde{x}}. \tag{26}$$

Since

$$\tilde{h}\frac{\partial \tilde{U}}{\partial \tilde{x}} = -\frac{2\tilde{W}}{\alpha} + O(\varepsilon^2), \tag{27}$$

we can write

$$\frac{\partial \tilde{h}\tilde{B}}{\partial \tilde{t}} + \varepsilon \frac{\partial \tilde{h}\tilde{U}\tilde{B}}{\partial \tilde{x}} = \sqrt{\tilde{h}}\left(2\tilde{h}\frac{\partial \tilde{W}}{\partial \tilde{x}} + \varepsilon\frac{3}{\alpha}\tilde{W}\tilde{S}\right) + O(\varepsilon^3). \tag{28}$$

With the definition (10) of S and the relation (12), we obtain the evolution equation for B in conservative form

$$\frac{\partial \tilde{h}\tilde{B}}{\partial \tilde{t}} + \frac{\partial}{\partial \tilde{x}}\left(\varepsilon\tilde{h}\tilde{U}\tilde{B} - 2\tilde{h}^{3/2}\tilde{W}\right) = O(\varepsilon^3). \tag{29}$$

1.2 Final set of equations

Finally, going back to the dimensional form, we obtain the following system :

$$\frac{\partial h}{\partial t} + \frac{\partial hU}{\partial x} = 0 \tag{30}$$

$$\frac{\partial hU}{\partial t} + \frac{\partial}{\partial x}\left(hU^2 + \frac{gh^2}{2} + hP\right) = -gh\frac{\partial z_b}{\partial x} \tag{31}$$

$$\frac{\partial hW}{\partial t} + \frac{\partial hUW}{\partial x} = \frac{3}{2}P + \frac{\alpha - 1}{2\alpha}gh^{3/2}\frac{\partial B}{\partial x} \tag{32}$$

$$\frac{\partial hP}{\partial t} + \frac{\partial hUP}{\partial x} = -a^2\left(2W + \alpha h\frac{\partial U}{\partial x}\right) \tag{33}$$

$$\frac{\partial hB}{\partial t} + \frac{\partial}{\partial x}\left(hUB - 2h^{3/2}W\right) = 0 \tag{34}$$

This system admits the following exact energy conservation:

$$\frac{\partial he}{\partial t} + \frac{\partial}{\partial x}\left(hUe + \frac{gh^2}{2}U + hPU + \Pi'\right) = 0\,, \tag{35}$$

with the energy:

$$e = \frac{U^2}{2} + \frac{2}{3\alpha}W^2 + \frac{gh}{2} + gz_b + \frac{P^2}{2\alpha a^2} + \frac{\alpha - 1}{6\alpha^2}gB^2\,, \tag{36}$$

and

$$\Pi' = -\frac{2}{3}\frac{\alpha - 1}{\alpha^2}gh^{3/2}WB. \tag{37}$$

This system is hyperbolic if $\alpha \geqslant 1$, and admits the following eigenvalues:

$$\lambda_1 = U\,, \tag{38}$$

$$\lambda_{2,3} = U \pm \sqrt{gh\frac{\alpha - 1}{\alpha}}\,, \tag{39}$$

$$\lambda_{4,5} = U \pm \sqrt{gh + P + \alpha a^2}\,. \tag{40}$$

Since the term $\partial(hUW)/\partial x$ is included in the model, this system admits the same non-linearities as the Serre-Green-Naghdi (in the limit $a \to \infty$). The moderate non-linearity assumption and the hypothesis α close to 1 only impact the terms involved in the improvement of dispersive properties. Moreover, since the neglected terms are non-linear, the dispersive properties are the same as in [52]. More explicitly, linearizing the system (30)–(34) around the constant state $h = h_0$, $U = U_0 = 0$, $P = P_0 = 0$, $W = W_0 = 0$, $B = B_0 = 0$ in the case of a flat horizontal bottom ($z_b = 0$) and looking for solutions under the form of monochromatic waves $\mathrm{e}^{i(kx - \omega t)}$, we obtain the following dispersion relation:

$$\frac{M_0^2}{3}\tilde{\omega}^4 - \tilde{\omega}^2\left[1 + \frac{\tilde{k}^2}{3}\left(\alpha + \frac{2\alpha - 1}{\alpha}M_0^2\right)\right] + \tilde{k}^2\left[1 + \tilde{k}^2\frac{\alpha - 1}{3}\left(1 + \frac{M_0^2}{\alpha}\right)\right] = 0 \tag{41}$$

where $\tilde{\omega} = \omega\sqrt{h_0/g}$ and $\tilde{k} = kh_0$. Note that in the limit $a \to +\infty$ ($M_0 \to 0$) we exactly recover the dispersion relation obtained in [4], for which the optimal value $\alpha = 1.159$ has been found. This value will be used in our numerical simulations (we refer to [52] for an exhaustive study of the influence of this parameter in the present context).

1.3 Soliton solution

The system (30)–(34) admits soliton solutions in the case of a flat bottom. Looking for solutions propagating at constant velocity c, we eventually fall on the following ODE system (see Appendix 4.1 for details):

$$\begin{cases} \dfrac{\mathrm{d}h}{\mathrm{d}\xi} = F(h,P,W) \\ \dfrac{\mathrm{d}P}{\mathrm{d}\xi} = a^2\left(-\dfrac{2W}{m} + \dfrac{\alpha}{h}F(h,P,W)\right) \\ \dfrac{\mathrm{d}W}{\mathrm{d}\xi} = \dfrac{3}{2}\dfrac{1}{m-h\theta}\left(P + \theta W F(h,P,W)\right) \end{cases} \tag{42}$$

Above, the function F is defined as:

$$F(h,P,W) = \frac{2a^2W}{m}\left(g - \frac{m^2}{h^3} + \frac{P}{h} + \frac{a^2\alpha}{h}\right)^{-1}, \tag{43}$$

where $m = h(U-c)$ is a constant quantity, and $\theta(h) = \dfrac{gh^2}{m}\dfrac{\alpha-1}{\alpha}$. The quantity B is deduced from W through the relation:

$$K = B - \frac{2h^{3/2}W}{m}, \tag{44}$$

where K is a constant. It should be remarked that if $\alpha = 1$, then $\theta = 0$ and we exactly recover the ODE system obtained for the classical soliton obtained in [52].

The soliton solution calculated with the system (42) is compared to the experimental results of Daily & Stephan (1952) [11]. The velocities of the calculated solitons are defined in dimensionless form by the Froude number $\overline{F} = |m|/\sqrt{gh_\infty^3} = c/\sqrt{gh_\infty}$, where h_∞ is the depth for $\xi \to \pm\infty$ and c the celerity of the soliton. The parameters used for these calculations are chosen in order to obtain the same amplitudes as the solitons generated in the experiments. As a result, the celerities of the calculated soliton are higher by 1 to 2.5 % than the celerities measured in the experiments. This is the same as in the case of the Serre-Green-Naghdi model. The celerities of the solitons calculted with the system (42) are almost the same as the celerities of the Serre-Green-Naghdi system. Reciprocally, if the parameters of the calculations are chosen in order to obtain the same celerity, the amplitude of the soliton is slightly underestimated in the same way as with the Serre-Green-Naghdi system. The four simulations are presented in Figure 2 with the experimental results (black dots), the soliton of Serre-Green-Naghdi ($\alpha = 1$) (blue curve) and the soliton obtained with the system (42) and $\alpha = 1.159$ (red curve). The values of the dimensionless amplitude, defined by $(h - h_\infty)/h_\infty$, are 0.232, 0.35, 0.493 and 0.60 for the figures 2(a), 2(b), 2(c) and 2(d) respectively. It is well-known that the Serre-Green-Naghdi soliton is slightly wider than an experimental soliton. The present system also gives a soliton which is slightly too wide, but the agreement is a little bit better than for the Serre-Green-Naghdi model, especially for the large amplitudes. Therefore, the improvement of the dispersive properties also improves the soliton profile even if there is still a small discrepancy.

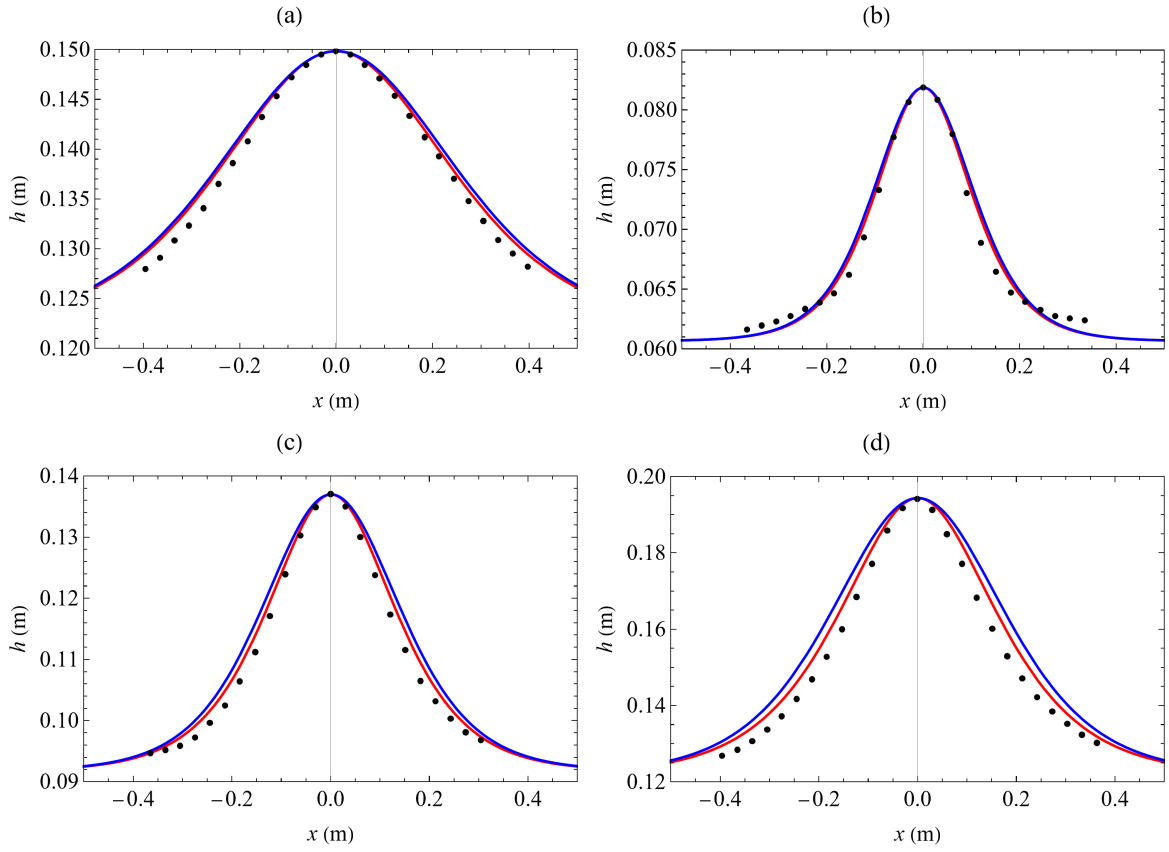

Figure 2: Comparison between the soliton profiles calculated with (42) and $\alpha = 1.159$ (red curves), the soliton profiles of the Serre-Green-Naghdi system ($\alpha = 1$) (blue curves) and the experimental results of Daily & Stephan (1952) [11] (black dots) for a dimensionless amplitude of 0.232 (a), 0.35 (b), 0.493 (c) and 0.60 (d).

2 Numerical approach

Going back to the system of equations (30) - (34), we construct a numerical scheme relying on the following splitting. The first step is simply made of the Shallow Water system with topography, supplemented by three passive transport equations:

$$\frac{\partial h}{\partial t} + \frac{\partial hU}{\partial x} = 0 \tag{45}$$

$$\frac{\partial hU}{\partial t} + \frac{\partial}{\partial x}\left(hU^2 + \frac{gh^2}{2}\right) = -gh\frac{\partial z_b}{\partial x} \tag{46}$$

$$\frac{\partial hW}{\partial t} + \frac{\partial hUW}{\partial x} = 0 \tag{47}$$

$$\frac{\partial hP}{\partial t} + \frac{\partial hUP}{\partial x} = 0 \tag{48}$$

$$\frac{\partial hB}{\partial t} + \frac{\partial hUB}{\partial x} = 0 \tag{49}$$

Recalling that e is given by (36), the corresponding energy equation is:

$$\frac{\partial he}{\partial t} + \frac{\partial}{\partial x}\left[\left(e + \frac{gh}{2}\right)hU\right] = 0\,. \tag{50}$$

The second part of the splitting contains the dispersive components of the system and involves the relaxation parameter a. This step will thus be called *acoustic* part in the following, and takes the form:

$$\frac{\partial h}{\partial t} = 0 \tag{51}$$

$$\frac{\partial hU}{\partial t} + \frac{\partial hP}{\partial x} = 0 \tag{52}$$

$$\frac{\partial hW}{\partial t} = \frac{3}{2}P + \frac{\alpha - 1}{2\alpha}gh^{3/2}\frac{\partial B}{\partial x} \tag{53}$$

$$\frac{\partial hP}{\partial t} = -a^2\left(2W + \alpha h\frac{\partial U}{\partial x}\right) \tag{54}$$

$$\frac{\partial hB}{\partial t} = \frac{\partial}{\partial x}\left(2h^{3/2}W\right) \tag{55}$$

This sub-system admits the following energy conservation equation:

$$\frac{\partial he}{\partial t} + \frac{\partial}{\partial x}\left(hPU + \Pi'\right) = 0\,. \tag{56}$$

From this, the objective is to propose a numerical approach able to ensure a discrete counterpart of the energy equations specific to each step, namely (50) and (56). The numerical treatment of each of these two parts is addressed separately in the two next sections. Before going further, we need to introduce the main notations employed to define the discrete operators used throughout the paper, as well as elementary estimates and duality formulas. In what follows, we will denote Δt the time step and consider a

regular grid implying cells of size Δx, referred to by $K \in \mathbb{Z}$. First, for any sequence of scalar interface quantity $(b_{K+1/2})_{K\in\mathbb{Z}}$, we define the centred operator:

$$\partial_K b = \frac{1}{\Delta x}\left(b_{K+1/2} - b_{K-1/2}\right) , \tag{57}$$

with the specific notation $\partial_K^c b$ when the interface quantities correspond to the half sum at the level of the two cells involved, that is:

$$\partial_K^c b = \frac{1}{\Delta x}\left(\bar{b}_{K+1/2} - \bar{b}_{K-1/2}\right) , \tag{58}$$

where $\bar{b}_{K+1/2} = \frac{1}{2}(b_K + b_{K+1})$. We also introduce the notation $[b]_{K+1/2} = \frac{1}{2}(b_{K+1} - b_K)$, so that $b_K = \bar{b}_{K+1/2} - [b]_{K+1/2} = \bar{b}_{K-1/2} + [b]_{K+1/2}$. These two definitions extend to multiple interface sequences by considering the difference of term to term interface products, leading to:

$$\partial_K(a,b) = \frac{1}{\Delta x}\left(a_{K+1/2}b_{K+1/2} - a_{K-1/2}b_{K-1/2}\right) . \tag{59}$$

We also define the discrete upwind derivative, for any collocated sequence of scalars $(a_K)_{K\in\mathbb{Z}}$:

$$\partial_K^{up}(a,b) = \frac{1}{\Delta x}\left(\mathcal{F}_{K+1/2} - \mathcal{F}_{K-1/2}\right) , \tag{60}$$

where $\mathcal{F}_{K+1/2} = a_K b^+_{K+1/2} + a_{K+1}b^-_{K+1/2}$, and $w^+ = \frac{1}{2}(w + |w|)$, $w^- = \frac{1}{2}(w - |w|)$. Equipped with these notations, we now focus on the first step of the splitting.

2.1 Hyperbolic subsystem

The first system (45)–(49) has a hyperbolic structure and can be numerically integrated on the basis of any approach for the Shallow-Water equations with topography source term. Keeping in mind energy stability issues, the method should rely on a method able to ensure entropy stability. Note that the variables W, P and B satisfy passive transport equations and are not a particular threat regarding the discrete energy balance. Among the fully explicit schemes available in the literature, a first example could be the fully entropic hydrostatic reconstruction scheme proposed in [2] for instance (see also the recent works [12], [32], [53]). We here chose to use a recent version of the explicit CPR scheme initially proposed in [10] (see also [48] for a first IMEX approach in the multi-layer case), details of which are available in [18]. Denoting the scalar potential $\phi = g(h + z_b)$, this approach relies on the following non-conservative rewriting of the momentum equation (46):

$$\frac{\partial hU}{\partial t} + \frac{\partial\left(hU^2\right)}{\partial x} + h\frac{\partial \phi}{\partial x} = 0 .$$

From this, the scheme for the hyperbolic part is:

$$\begin{cases} h_K^{n+1} = h_K^n - \Delta t \partial_K(q^*) , \\ (hU)_K^{n+1} = (hU)_K^n - \Delta t \partial_K^{up}(U, q^*) - \Delta t h_K^n \partial_K(\phi^*) , \\ (hW)_K^{n+1} = (hW)_K^n - \Delta t \partial_K^{up}(W, q^*) , \\ (hP)_K^{n+1} = (hP)_K^n - \Delta t \partial_K^{up}(P, q^*) , \\ (hB)_K^{n+1} = (hB)_K^n - \Delta t \partial_K^{up}(B, q^*) . \end{cases} \tag{61}$$

Referring to formulas (57) and (60), we only need to specify $q^*_{K+1/2}$ and $\phi^*_{K+1/2}$ to characterize the discrete operators. We set:

$$q^*_{K+1/2} = (\overline{hU})_{K+1/2} - \Pi_{K+1/2}\,, \tag{62}$$

and

$$\phi^*_{K+1/2} = \bar{\phi}_{K+1/2} - \Lambda_{K+1/2}\,, \tag{63}$$

where we recall that the superscript "$-$" refers to the mean interface value taken at time n (the scheme being totally explicit, the time indice will be omitted when no confusion is possible in the following). The quantities $\Pi_{K+1/2}$ and $\Lambda_{K+1/2}$ govern the numerical viscosity of the scheme, and are defined as:

$$\Pi_{K+1/2} = 2c_p\lambda(\overline{h\nu})_{K+1/2}[\phi]_{K+1/2}\,, \tag{64}$$

$$\Lambda_{K+1/2} = 2gc_\ell\lambda[hU]_{K+1/2}\,, \tag{65}$$

where c_p, c_ℓ are positive constants and $\lambda = \Delta t/\Delta x$. As stated in [18], the scheme is energy dissipative under the following conditions:

- The time step is defined according to the following interface CFL condition:

$$\lambda(\mathfrak{u}^*_{K+1/2} + \widehat{\mathfrak{c}}_{K+1/2}) \leqslant 1/4\,, \tag{66}$$

  where $\mathfrak{u}^*_{K+1/2} = \dfrac{1}{2}\left(|\overline{hU}_{K+1/2}| + \dfrac{1}{2g}\gamma\bar{c}_e|[\phi]_{K+1/2}|\right)/\widehat{h}_{K+1/2}$, with $\widehat{h}_{K+1/2} = \max(h^n_K, h^n_{K+1})$, and $\widehat{\mathfrak{c}}_{K+1/2} = \max\left(\mathfrak{c}_K, \mathfrak{c}_{K+1}\right)$ where $\mathfrak{c}_K = \sqrt{gh^n_K}$.

- The constants c_p, c_ℓ have to satisfy the following bounds:

$$c_p, c_\ell \in [r^-, r^+] \quad , \quad \text{with } r^\pm(\vartheta) = \frac{1 \pm \sqrt{1-\vartheta}}{\vartheta/2}\,, \tag{67}$$

  where $\vartheta = 16\lambda^2 g(\overline{h\nu})_{K+1/2}$. Note that we have $\lim\limits_{\vartheta\to 0} r^-(\vartheta) = 1$, $r^\pm(1) = 2$ and $\lim\limits_{\vartheta\to 0} r^+(\vartheta) = +\infty$. The function $\vartheta \mapsto r^-(\vartheta)$ being increasing and $\vartheta \mapsto r^+(\vartheta)$ decreasing on the interval $[0,1]$, we get that the value $c_p = c_\ell = 2$ is always admissible, independently from K. Note also the possibility of taking c_p, c_ℓ close to 1 by diminishing ϑ (that is the time step). Finally, the local parameter ν implied in the interface term $(\overline{h\nu})_{K+1/2}$ in (64) is defined as $\nu_K = \dfrac{1}{1-4\lambda\mathfrak{u}_K}$ where $\mathfrak{u}_K = \max(\mathfrak{u}^*_{K-1/2}, \mathfrak{u}^*_{K+1/2})$, and can be roughly estimated by $\nu_K \leqslant 1 + (Fr)_K$, where $(Fr)_K = \dfrac{\mathfrak{u}_K}{\mathfrak{c}_K}$ stands for a local Froude number.

More explicitely, defining the local potential and kinetic energies provided by the scheme as:

$$\mathcal{E}^n_K = gh^n_K\left(\frac{h^n_K}{2} + (z_b)_K\right) \quad , \quad \mathcal{K}^n_K = \frac{1}{2}h^n_K\left(U^n_K\right)^2\,, \tag{68}$$

and the energy contributions associated with the other variables:

$$\mathcal{W}^n_K = \frac{2}{3\alpha}h^n_K\left(W^n_K\right)^2 \quad , \quad \mathcal{P}^n_K = \frac{1}{2\alpha a^2}h^n_K\left(P^n_K\right)^2 \quad , \quad \mathcal{B}^n_K = \frac{\beta}{2}h^n_K\left(B^n_K\right)^2\,, \tag{69}$$

with $\beta = g\dfrac{\alpha-1}{3\alpha^2}$, we recover under the conditions mentioned above a discrete counterpart of (50) through an estimation of the form:

$$E_K^{n+1} - E_K^n + \Delta t\, \mathfrak{d}_K\left(e + \frac{1}{2}gh, hU\right) \leqslant 0\,, \tag{70}$$

where $E_K^n = \mathcal{E}_K^n + \mathcal{K}_K^n + \mathcal{W}_K^n + \mathcal{P}_K^n + \mathcal{B}_K^n$ is the local energy of the system at time n at the level of the cell K. The numerical energy flux is given by:

$$\mathfrak{d}_K\left(e + \frac{1}{2}gh, hU\right) = \widetilde{\partial_K^{up}}\left(\frac{1}{2}u^2, q^*\right) + \widetilde{\partial_K}(\phi, q^*) + \partial_K^{up}\left(\frac{2}{3\alpha}W^2 + \frac{1}{2\alpha a^2}P^2 + \frac{\beta}{2}B^2, q^*\right).$$

Above, the upwind fluxes ∂_K^{up} are defined by (60), and the operators $\widetilde{\partial_K^{up}}$ and $\widetilde{\partial_K}$ refer to consistent fluxes which leading part is given by (59), (60), subject to smaller order contributions (we refer to [18] for an explicit form of these correction terms).

2.2 Acoustic subsystem

We now turn to the numerical scheme associated with the acoustic part (52)–(55), for which the scheme we consider is the following:

$$\begin{cases} U_K^{n+1} = U_K^n - \dfrac{\Delta t}{h_K^n}\partial_K^c(hP^{n+1})\,, \\ W_K^{n+1} = W_K^n + \Delta t\dfrac{3}{2}\dfrac{P_K^{n+1}}{h_K^n} + \Delta t\dfrac{\alpha-1}{2\alpha}g\sqrt{h_K^n}\partial_K B^*\,, \\ P_K^{n+1} = P_K^n - \Delta t a^2\left[2\dfrac{W_K^{n+1}}{h_K^n} + \alpha\partial_K U^*\right], \\ B_K^{n+1} = B_K^n + \dfrac{\Delta t}{h_K^n}\partial_K^c\left(2h^{3/2}W^{n+1}\right). \end{cases} \tag{71}$$

Since the water height does not evolve through the acoustic step, we will denote $h_K = h_K^n = h_K^{n+1}$ for simplification purposes. We set:

$$\partial_K U^* = \frac{1}{\Delta x}\left(U^*_{K+1/2} - U^*_{K-1/2}\right) \quad \text{with} \quad U^*_{K+1/2} = \bar{U}_{K+1/2} - \Gamma_{K+1/2}\,, \tag{72}$$

and

$$\partial_K B^* = \frac{1}{\Delta x}\left(B^*_{K+1/2} - B^*_{K-1/2}\right) \quad \text{with} \quad B^*_{K+1/2} = \bar{B}_{K+1/2} - \Theta_{K+1/2}\,. \tag{73}$$

Above, $\Gamma_{K+1/2}$ and $\Theta_{K+1/2}$ are governing numerical viscosity, with a role similar to (64) and (65) in the hyperbolic part. Also, as will be seen later, these terms can actually be chosen such that the present scheme can be solved totally explicitly. In what follows, we will introduce the following notations:

$$\zeta_K = \frac{3}{2}\frac{P_K^{n+1}}{h_K^n} + \frac{\alpha-1}{2\alpha}g\sqrt{h_K^n}\partial_K B^*\,, \tag{74}$$

and

$$\xi_K = 2\frac{W_K^{n+1}}{h_K} + \alpha\partial_K U^*\,, \tag{75}$$

so that the discrete evolution of the variable W and P in (71) can be simply rewritten:

$$W_K^{n+1} = W_K^n + \Delta t \zeta_K \,. \tag{76}$$

$$P_K^{n+1} = P_K^n - \Delta t a^2 \xi_K \,, \tag{77}$$

Finally, in order to make the forthcoming formulations more compact, we set:

$$R_K^n = h_K P_K^n \qquad , \qquad S_K^n = -2(h_K)^{3/2} W_K^n \,. \tag{78}$$

We now give the main steps leading to the scheme stability. The proof of the following propositions are quite heavy and have been relegated to the Appendix 4.2 for the sake of readability. We start with the following general result:

Proposition 1. *Referring to notations (68), (69), consider* $E_K^n = \mathcal{E}_K^n + \mathcal{K}_K^n + \mathcal{W}_K^n + \mathcal{P}_K^n + \mathcal{B}_K^n$ *the local energy at time* n*. Then the following equality stands:*

$$E_K^{n+1} - E_K^n + \Delta t \widetilde{\partial_K^c} \left(R^{n+1}, U \right) + \Delta t \widetilde{\partial_K^c} \left(\beta S^{n+1}, B \right) = \mathbb{H}_K + \mathbb{G}_K \,, \tag{79}$$

where we recall that $\beta = g \dfrac{\alpha - 1}{3\alpha^2}$*, and where*

$$\mathbb{H}_K = \Delta t R_K^{n+1} \partial_K \Gamma + \frac{1}{2} h_K \left(U_K^{n+1} - U_K^n \right)^2 - \Delta t^2 \frac{a^2}{2\alpha} h_K \xi_K^2 \,, \tag{80}$$

$$\mathbb{G}_K = \Delta t \beta S_K^{n+1} \partial_K \Theta + \frac{1}{2} \beta h_K \left(B_K^{n+1} - B_K^n \right)^2 - \Delta t^2 \frac{2 h_K}{3\alpha} \zeta_K^2 \,, \tag{81}$$

and the discrete operator $\widetilde{\partial_K^c}$ *is defined by:*

$$\widetilde{\partial_K^c}(a,b) = \partial_K^c(a,b) - \partial_K \left([a], [b] \right) \,, \tag{82}$$

for any pair of collocated sequence of scalar quantities $(a_K)_{K \in \mathbb{Z}}, (b_K)_{K \in \mathbb{Z}}$*.*

Based on this, we now seek a control of the residuals $\mathbb{H}_K$ and $\mathbb{G}_K$. This leads to the following estimates:

Proposition 2. *Assume that the stabilisation term involved in (72) is given by:*

$$\Gamma_{K+1/2} = c_g \lambda \left(\overline{1/h} \right)_{K+1/2} [h P^n]_{K+1/2} \,. \tag{83}$$

Then, under the CFL condition:

$$\frac{\Delta t}{\Delta x} \sqrt{\alpha} a \leqslant \frac{1}{2\sqrt{\tau_{K+1/2}}} \qquad \textit{with} \qquad \tau_{K+1/2} = \overline{h}_{K+1/2} \left(\overline{1/h} \right)_{K+1/2} \,, \tag{84}$$

and assuming that c_g *satisfies the bounds (67):*

$$c_g \in [r^-, r^+] \quad , \quad \textit{with } r^{\pm}(\vartheta) = \frac{1 \pm \sqrt{1 - \vartheta}}{\vartheta/2} \,, \tag{85}$$

with this time $\vartheta = 4 \left(\dfrac{\Delta t}{\Delta x} \right)^2 a^2 \alpha \tau_{K+1/2}$*, we have:*

$$\mathbb{H}_K \leqslant \Delta t \mathcal{A}_K \,, \tag{86}$$

where $\mathcal{A}_K$ *is a residual flux term, seen as a bias on the leading flux* $\widetilde{\partial_K^c} \left(R^{n+1}, U \right)$ *involved in (79) (see formula (130) for an explicit formulation of this term).*

Proposition 3. *Assume that the stabilisation term (73) is given by:*

$$\Theta_{K+1/2} = -c_t \lambda \left(\overline{1/h}\right)_{K+1/2} [2h^{3/2} W^n]_{K+1/2} \,, \tag{87}$$

and note $\sigma_K = \sqrt{g h_K \left(\frac{\alpha - 1}{\alpha}\right)}$. *Then, under the CFL condition:*

$$\frac{\Delta t}{\Delta x} \sigma_{K+1/2} \leqslant \frac{1}{2\sqrt{\tau_{K+1/2}}} \qquad \text{with} \qquad \tau_{K+1/2} = \overline{h}_{K+1/2} \left(\overline{1/h}\right)_{K+1/2} , \tag{88}$$

$\sigma_{K+1/2} = \max(\sigma_K, \sigma_{K+1})$, *and assuming that* c_t *satisfies the bounds (67):*

$$c_t \in [r^-, r^+] \quad , \quad \text{with } r^{\pm}(\vartheta) = \frac{1 \pm \sqrt{1 - \vartheta}}{\vartheta/2} \,, \tag{89}$$

with $\vartheta = 4 \left(\frac{\Delta t}{\Delta x}\right)^2 \sigma_{K+1/2}^2 \tau_{K+1/2}$, *we have:*

$$\mathbb{G}_K \leqslant \Delta t \beta \mathcal{B}_K \,, \tag{90}$$

where $\mathcal{B}_K$ *is a bias on the leading flux* $\widetilde{\partial_K^c}(\beta S^{n+1}, B)$ *appearing in (79) (see (140)).*

We can now enounce the main stability result, as a direct consequence of the two previous propositions:

Proposition 4. *Under the hypothesis of Propositions 2 and 3, the acoustic scheme (71) satisfies the following energy estimate:*

$$E_K^{n+1} - E_K^n + \Delta t \widetilde{\partial_K^c}\left(R^{n+1}, U\right) + \Delta t \widetilde{\partial_K^c}\left(\beta S^{n+1}, B\right) \leqslant 0 \,, \tag{91}$$

with

$$\widetilde{\partial_K}\left(R^{n+1}, U\right) = \widetilde{\partial_K^c}\left(R^{n+1}, U\right) - \mathcal{A}_K \,,$$
$$\widetilde{\partial_K}\left(\beta S^{n+1}, B\right) = \widetilde{\partial_K^c}\left(\beta S^{n+1}, B\right) - \beta \mathcal{B}_K \,,$$

where $\mathcal{A}_K$ *and* $\mathcal{B}_K$ *are low order flux corrections (respectively given by (130), (140)). The discrete operators* $\widetilde{\partial_K^c}$ *are defined according to (82).*

Recalling that $R^{n+1} = hP^{n+1}$, $\beta S^{n+1} = -\frac{2}{3}\frac{\alpha - 1}{\alpha^2} g h^{3/2} W^{n+1}$, we thus get a discrete equivalent of (56). This concludes the discussion on the scheme stability.

Remark 1. *(Preservation of motionless steady stades). Due to the nature of the viscosity terms (64), (65) and (83), (87), it is easy to check that motionless steady states, characterized here by* $\phi = cte$, $U = 0$, $W = 0$, $P = 0$, $B = 0$, *are automatically preserved at the discrete level through both hyperbolic and acoustic steps.*

3 Numerical experiments

3.1 Implementation issues

As concerns numerical implementation, first note that the acoustic scheme can be reformulated in a fully explicit frame. Returning to (71), the strategy consists in computing W^{n+1} and P^{n+1} explicitly in a first step, before treating the two remaining equations. After basic calculations, we indeed get the following formulas:

$$W_K^{n+1} = W_K^n + \Delta t \left[\frac{3}{2h_K^n} \left(P_K^n - \Delta t^2 a^2 \alpha \partial_K U^* \right) + \frac{\alpha - 1}{2\alpha} g \sqrt{h_K^n} \partial_K B^* \right] / I_K^n \,,$$

and

$$P_K^{n+1} = P_K^n - \Delta t a^2 \left[\frac{2}{h_K^n} \left(W_K^n + \Delta t \frac{\alpha - 1}{2\alpha} g \sqrt{h_K^n} \partial_K B^* \right) + \alpha \partial_K U^* \right] / I_K^n \,,$$

with an implicitation coefficient given by $I_K^n = 1 + 3a^2 \Delta t^2 / (h_K^n)^2$. Regarding the time scheme, a second order Strang splitting is considered here. Note that the two stages involved in the numerical approach are governed by different time step conditions, given by (66) and (84) (which is much more restrictive than (88)). In particular, in order to benefit from the classical shallow water CFL condition issuing from the first step (which is not restricted by the parameter a), these two time scales are taken into account for a better efficiency. In practice, this implies a multi-stage resolution of the acoustic part based on the more restrictive time step Δt_{ac} obtained in (84). More precisely, denoting by Δt the time step issuing from the hyperbolic condition (66), we set $\Delta t_p = \Delta t / p$, where $p = \left\lceil \dfrac{\Delta t}{\Delta t_{ac}} \right\rceil + 1$, and consider the following time scheme:

$$\left\{ \begin{array}{ll} U_K^{(1)} & = \mathcal{S}_{hyp} \left(\dfrac{\Delta t}{2} \right) U_K^{(n)} \,, \\ U_K^{(2)} & = \left[\mathcal{S}_{ac}(\Delta t_p) \right]^p U_K^{(1)} \,, \\ U_K^{(n+1)} & = \mathcal{S}_{hyp} \left(\dfrac{\Delta t}{2} \right) U_K^{(2)} \,. \end{array} \right.$$

Above, $\mathcal{S}_{hyp}$ refers to the hyperbolic scheme (61) and $\mathcal{S}_{ac}$ refers to the acoustic system (71). This strategy allows a significant gain in calculation time, without compromising the order of the method. It is supplemented by a standard MUSCL procedure for a formal second order accuracy in space.

3.2 Propagation of a soliton on a flat bottom

Starting from the ODE system (42), an analytical solution can be computed assuming $h \longrightarrow h_\infty$, $U \longrightarrow 0$, $W \longrightarrow 0$, $P \longrightarrow 0$ and $B \longrightarrow 0$ as $\xi \longrightarrow \pm\infty$. Note that in this case the constant m (see (92)) can be prescribed imposing the relative Froude number $F_\infty := -m/\sqrt{g h_\infty^3}$, and the constant $K = B - 2h^{3/2} W/m$ connecting B to W is equal to zero. We consider here the propagation of a soliton defined by $h_\infty = 1\,\mathrm{m}$ and $F_\infty = 1.8$, centred in the domain $\Omega = [-50, 50]$. The computational domain is meshed with 2000 elements, and we take $a = 40\,\mathrm{m} \cdot \mathrm{s}^{-1}$, $\alpha = 1.159$. Periodic conditions are imposed at the

boundaries, leading to a period $P = 23.79739\,\mathrm{s}$ for the soliton to recover its initial position. We can observe on Fig. 3 the water height elevation of the numerical solution after two periods, compared to the initial solution. The wave amplitude is well reproduced and no significant phase shift can be observed. For the record, the loss of amplitude is of 0.6% and the phase shift is of 0.1% at this level of resolution ($L/\Delta x \approx 200$). Note that although the analytical solution is computed with $a = 1500\,\mathrm{m.s^{-1}}$, the value $a = 40\,\mathrm{m.s^{-1}}$ is amply sufficient here to reproduce the wave characteristics with a high level of accuracy. Note that all the terms implied in the local dissipation estimations (70) and (91) have been explicitly computed. We thus verified numerically that these inequalities were rigorously satisfied up to the error machine at first order.

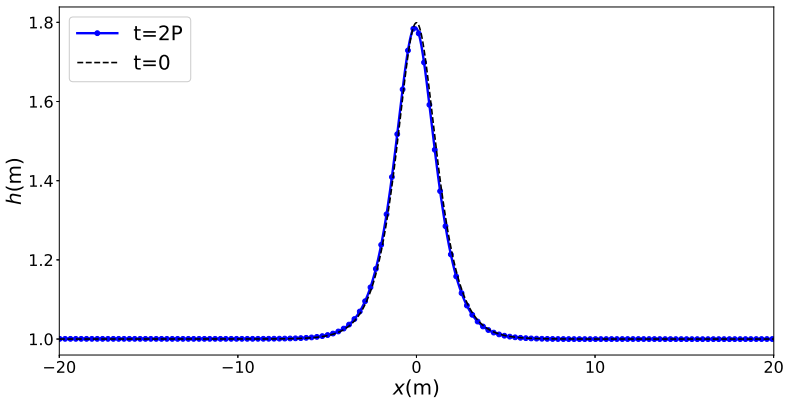

Figure 3: Soliton solution. Initial condition (*dashed lines*) vs. water height elevation after two periods (*plain lines*).

3.3 Waves train over a submerged bar

We now consider the classical set of experiments of Beji & Battjes [1], which aims at studying the deformations of wave trains propagating over a submerged bar. The experimental set-up implies a 37.7 m long rectangular basin, which bottom variations correspond to a trapezoidal bar of 1/20 upslope and 1/10 downslope. In the experiment the reference water height in the deep part of the channel is fixed to 0.4 m, leading to the configuration depicted in Fig. 4. The water elevation has been recorded at eight wave gauges, the first one being located at the foot of the bar, and the other ones being regularly spaced along the top part and the rear side. Many series of experiments have been run, implying either breaking and non-breaking waves in the case of regular and irregular waves, details of which can be found in [1]. Since the objective here is to assess the dispersive properties and the energy-dissipative features of the scheme, we only focus on the non-breaking cases, and refer to [17], [30] for instance for recent works related to wave-breaking issues.

When an incident wave encounters the upward part of the bar, it shoals and steepens, which generates high harmonics. These higher-harmonics are then freely released on the downward slope, and become deep-water waves behind the bar. These dynamics are not easy to capture and this test case is proving to be a discriminating criterion for attesting to the dispersive and non-linear properties of water waves models.

As regards the treatment of boundary conditions, a relaxation zone of 5 m as been added at the inlet boundary, allowing to progressively transit from an imposed profile to the numerical solution inside the computational domain. In each of the cases considered here, according to the experimental configuration, a train of sinusoidal waves of amplitude $A = 0.01\,\mathrm{m}$ has been generated, based on a solution of the linearized system. A similar protocol has been implemented at the outlet boundary to absorb outgoing waves and prevent from any reflection phenomena. According to this, the computational domain is set to $\Omega = [-10, 30]$.

We first consider the case of a frequency of 0.4 Hz. The numerical model has been run with 4000 elements, with a correction coefficient $\alpha = 1.159$ and an artificial sound velocity $a = 20\,\mathrm{m.s}^{-1}$. Note that grid convergence is reached at this level of resolution. We also point that, as reported in the experimental study and many works in the literature, the standard dispersive properties of the Serre-Green-Naghdi model show their limitations in this configuration and need to be improved (see for instance [52]). Comparisons between experimental and numerical results at gauges 1,3,5,6,7 and 8 are available in Fig. 5, showing a very good level of agreement, qualitatively similar to the complete compressible model [52]. Also, although it may seem relatively small in relation to its physical value,

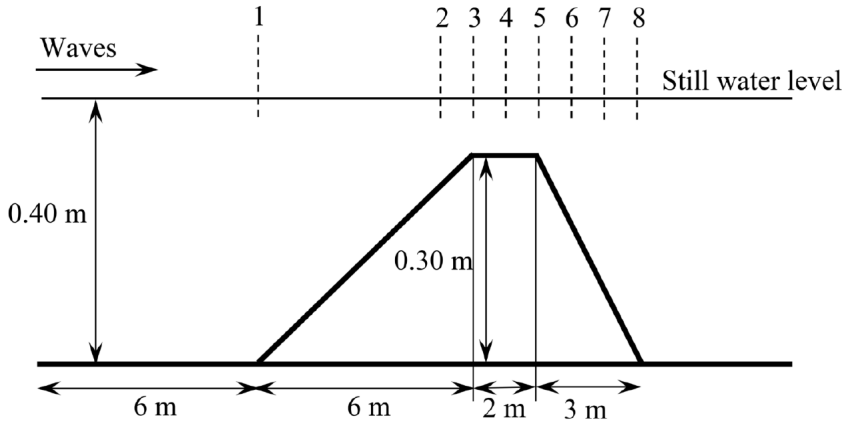

Figure 4: Test case of Beji & Battjes [1]. Sketch of the experimental set-up.

we found that this order of magnitude for a was already sufficient to provide accurate results, and we did not observe any clear improvement brought by its increase (see Fig. 8).

We now turn to the case 0.1 Hz. Again the computational domain is discretized with 4000 elements and the value $\alpha = 1.159$ is taken. The sound velocity is set to $a = 20\,\mathrm{m.s}^{-1}$. Fig. 7 provides the comparisons between experimental and numerical results at gauges 1,3,5,6,7 and 8, and exhibit a good agreement. As noticed in [52], even more accurate dispersive properties would be necessary to have a better agreement at the two last gauges, which is part of future works. This can be reached introducing a richer set of free parameters in the system (as done in [8] for instance), increasing the number of variables, or even considering a two-layer extension. However in the present frame, in addition to their intrinsic specificities, these methods must be implemented without compromising the hyperbolicity of the model and while preserving an exact energy balance, which is, at first sight, not a native feature of these strategies. The impact of the calibration of

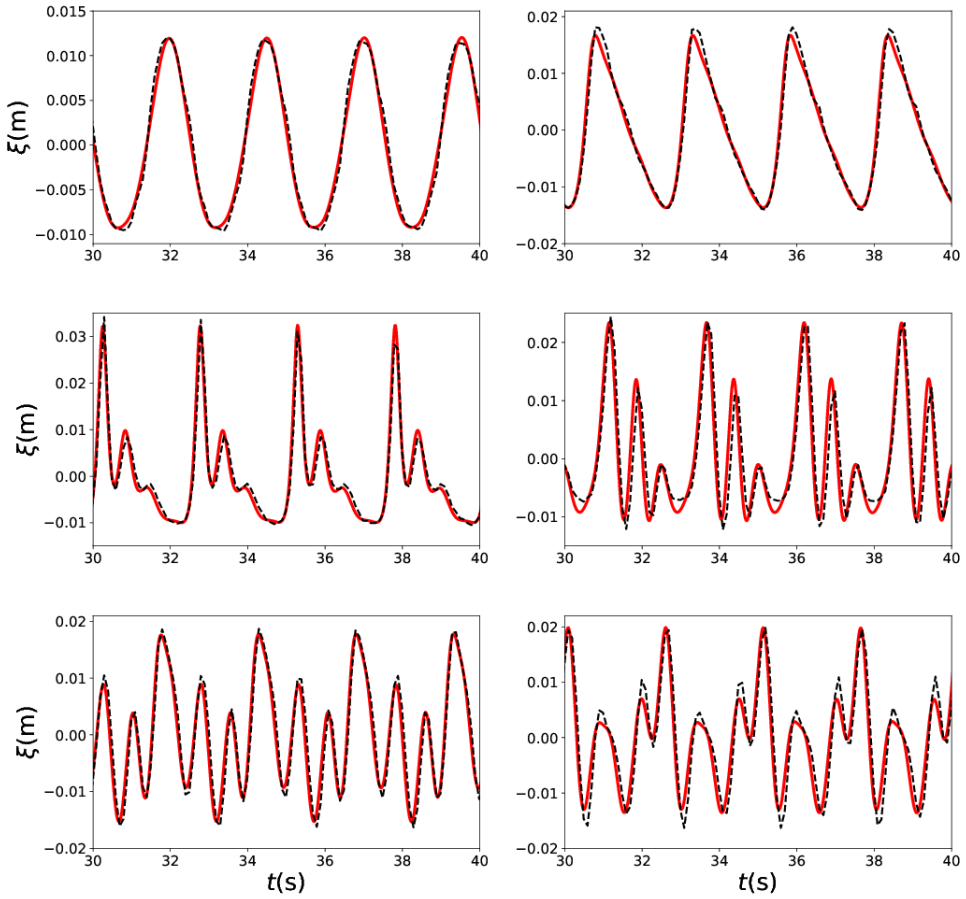

Figure 5: Comparisons of the model with improved dispersive properties ($\alpha = 1.159$) (*plain lines*) with the experimental results (*dashed lines*) in the case 0.4 Hz - Free surface elevation with respect to the reference level. From top to bottom and left to right: wave gauges 1,3,5,6,7 and 8.

the sound velocity a can be assessed through Fig. 8, from which we can observe that the value $a = 20\,\mathrm{m.s}^{-1}$ is already sufficient to properly approach the limit model. As in the previous test, it has to be noted that the local energy estimates (70) and (91) have been systematically satisfied at first order, attesting of the dissipative features of the scheme even in the presence of topography.

Conclusion

We derived a hyperbolic model for the propagation of dispersive waves enjoying improved dispersive properties and an exact conservation of energy. The system is derived under a moderate non-linearity hypothesis and assuming a correction coefficient close to 1. These scale hypothesis only affect the part of the system dedicated to improving dispersive properties, allowing to recover the same non-linearities as those of the classical Serre-

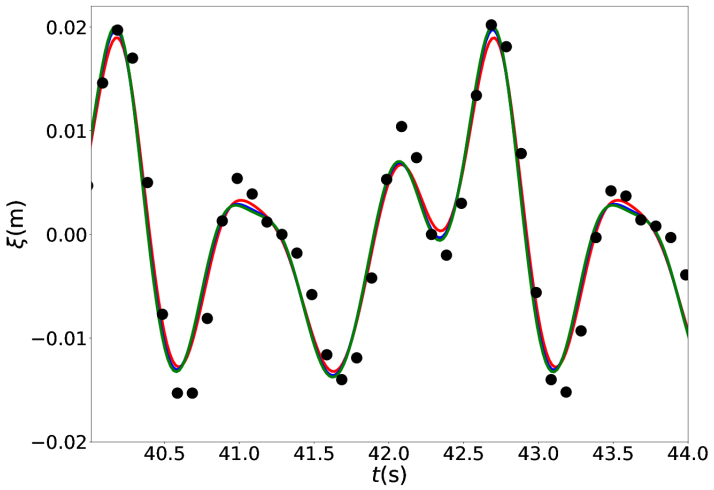

Figure 6: Comparisons of the model with improved dispersive properties ($\alpha = 1.159$) (*plain lines*) with the experimental results (*dots*) in the case 0.4 Hz aud wage gauge 8 - Free surface elevation with respect to the reference level. $a = 10\,\mathrm{m.s^{-1}}$ (*red curve*), $a = 20\,\mathrm{m.s^{-1}}$ (*blue curve*), $a = 40\,\mathrm{m.s^{-1}}$ (*green curve*).

Green-Naghdi equations. We have shown that this system admits a family of soliton solutions, which turn out to be closer to the experimental measurements than the classical SGN solitons. Extending the recent explicit *low-Froude* CPR approaches ([48],[10]), an efficient and low-diffusive numerical scheme has been proposed, which main feature is to ensure stability through discrete energy dissipation. The numerical approach relies on a splitting between the hyperbolic and the acoustic parts, and stability is obtained by establishing a discrete counterpart of the energy balance specific to each stage. In particular, the hyperbolic part of the splitting is not impacted by the sound velocity, which allows to involve the classical hyperbolic time step emanating from the Shallow Water equations and to improve computational efficiency. Numerical experiments have been proposed to highlight the dispersive properties of the method and the dissipative nature of the scheme. In accordance with the observations made in [52], we have shown that the value of the sound velocity a could be taken much lower than its physical value, leading to significant computational savings. In parallel of finding relevant strategies to provide even better dispersive properties in the present frame, the two dimensional extension, as well as the inclusion of all topography terms is left for future works. Also, the justification of the model is on ongoing work, on the basis on the recent developments made in [14].

Acknowledgments

Arnaud Duran acknowledges financial support from the French National Research Agency project MOTIONS, grant ANR-23-CE56-0006-02 and from the SHOM research contract N°21CP05.

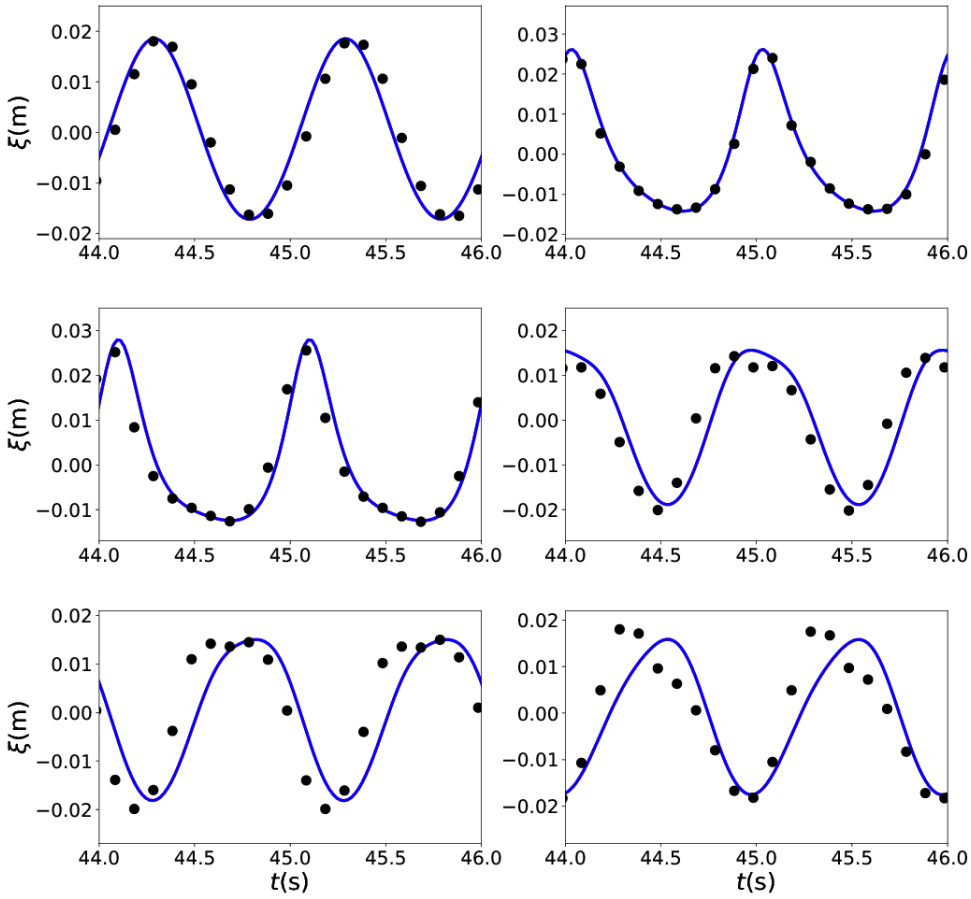

Figure 7: Comparisons of the model with improved dispersive properties ($\alpha = 1.159$) (*plain lines*) and experimental results (*dotted lines*) in the case 0.1 Hz - Free surface elevation with respect to the reference level. From top to bottom and left to right: wave gauges 1,3,5,6,7 and 8.

4 Appendix

4.1 Soliton solution

We look for solutions of the system (30)-(34) as function of the variable $\xi = x - ct$, where c is a constant. The mass equation gives a first constant:

$$m = h(U - c)\,. \tag{92}$$

Then, the momentum equation gives:

$$\frac{\mathrm{d}}{\mathrm{d}\xi}\left(-hcU + hU^2 + \frac{gh^2}{2} + hP\right) = 0\,,$$

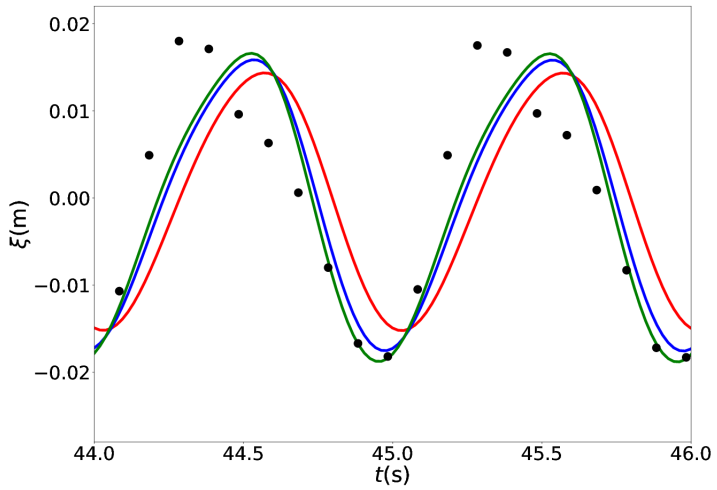

Figure 8: Comparisons of the model with improved dispersive properties ($\alpha = 1.159$) (*plain lines*) with the experimental results (*dots*) in the case 0.1 Hz aud wage gauge 8 - Free surface elevation with respect to the reference level. $a = 10\,\mathrm{m.s^{-1}}$ (*red curve*), $a = 20\,\mathrm{m.s^{-1}}$ (*blue curve*), $a = 40\,\mathrm{m.s^{-1}}$ (*green curve*).

that is $Um + \dfrac{gh^2}{2} + hP = cte$. Using (92), we have $Um = m^2/h + cte$, so that we can identify a second constant quantity:

$$I = \frac{m^2}{h} + \frac{gh^2}{2} + hP\,. \tag{93}$$

Note that the energy equation can be rewritten:

$$\frac{\mathrm{d}}{\mathrm{d}\xi}\left(me + \Pi U + \Pi'\right) = 0\,,$$

where $\Pi = \dfrac{gh^2}{2} + hP$. Using (93), we obtain, after some basic calculations:

$$\Pi U = m\left(\frac{gh}{2} + P\right) - c\frac{m^2}{h} + cte\,.$$

On the other hand the first term of (36) can be written as follows:

$$\frac{1}{2}U^2 = \frac{1}{2}\left(\frac{m}{h} + c\right)^2 = \frac{1}{2}\frac{m^2}{h^2} + \frac{cm}{h} + cte\,.$$

Hence we have $me + \Pi U + \Pi' = mJ + cte$, where J corresponds to a third constant:

$$J = \frac{1}{2}\frac{m^2}{h^2} + \frac{2}{3\alpha}W^2 + gh + \frac{P^2}{2\alpha a^2} + P + \frac{\alpha - 1}{6\alpha^2}gB^2 + \frac{\Pi'}{m} \tag{94}$$

Then, noting that from equation (34) we have $\frac{\mathrm{d}}{\mathrm{d}\xi}(mB) = \frac{\mathrm{d}}{\mathrm{d}\xi}\left(2h^{3/2}W\right)$, we can extract a fourth constant K connecting B to W:

$$K = B - \frac{2h^{3/2}W}{m}\,. \tag{95}$$

In particular, this leads to:

$$\frac{\mathrm{d}B}{\mathrm{d}\xi} = \frac{2h^{3/2}}{m}\frac{\mathrm{d}W}{\mathrm{d}\xi} + \frac{3W\sqrt{h}}{m}\frac{\mathrm{d}h}{\mathrm{d}\xi}\,. \tag{96}$$

As a result, equation (32) can be written as:

$$\frac{\mathrm{d}W}{\mathrm{d}\xi}\left(m - \frac{\alpha-1}{\alpha}\frac{gh^3}{m}\right) = \frac{3}{2}P + \frac{3}{2}\frac{\alpha-1}{\alpha}\frac{gh^2W}{m}\frac{\mathrm{d}h}{\mathrm{d}\xi}\,,$$

Assuming $m \neq \frac{\alpha-1}{\alpha}\frac{gh^3}{m}$, we set

$$\theta(h) = \frac{gh^2}{m}\frac{\alpha-1}{\alpha} \quad , \quad \phi(h) = \frac{3}{2}\frac{1}{m - h\theta(h)}\,, \tag{97}$$

and the previous equation rewrites:

$$\frac{\mathrm{d}W}{\mathrm{d}\xi} = \phi P + \phi\theta W\frac{\mathrm{d}h}{\mathrm{d}\xi}\,. \tag{98}$$

From (92), we have $\frac{\mathrm{d}U}{\mathrm{d}\xi} = -\frac{m}{h^2}\frac{\mathrm{d}h}{\mathrm{d}\xi}$, and exploit the equation (33) to obtain:

$$\frac{\mathrm{d}P}{\mathrm{d}\xi} = -\frac{2a^2W}{m} + \frac{a^2\alpha}{h}\frac{\mathrm{d}h}{\mathrm{d}\xi}\,. \tag{99}$$

Finally, with (96) and (98), we can also express the derivative of B in terms of $\frac{\mathrm{d}h}{\mathrm{d}\xi}$:

$$\frac{\mathrm{d}B}{\mathrm{d}\xi} = \frac{2h^{3/2}}{m}\phi P + \left(\frac{2h^{3/2}}{m}\phi\theta W + \frac{3W\sqrt{h}}{m}\right)\frac{\mathrm{d}h}{\mathrm{d}\xi}\,. \tag{100}$$

We now consider the following decomposition of the constant (94): $J = J_1 + J_2$ with

$$\begin{aligned} J_1 &= \frac{1}{2}\frac{m^2}{h^2} + \frac{2}{3\alpha}W^2 + gh + \frac{P^2}{2\alpha a^2} + P \\ J_2 &= \frac{\alpha-1}{6\alpha^2}gB^2 - \frac{2}{3}\frac{\alpha-1}{\alpha^2}\frac{gh^{3/2}WB}{m} \end{aligned} \tag{101}$$

Based on (99) and (98), we get, after several algebraic manipulations:

$$\frac{\mathrm{d}J_1}{\mathrm{d}\xi} = -\frac{2a^2W}{m} + \left(g - \frac{m^2}{h^3} + \frac{P}{h} + \frac{a^2\alpha}{h}\right)\frac{\mathrm{d}h}{\mathrm{d}\xi} + \mathcal{R} \tag{102}$$

with

$$\mathcal{R} = \frac{4}{3}\frac{WP}{\alpha m}\left(\phi m - \frac{3}{2}\right) + \frac{4}{3\alpha}W^2\phi\theta\frac{\mathrm{d}h}{\mathrm{d}\xi}\,. \tag{103}$$

The next step is to show that $\mathcal{R} + \dfrac{\mathrm{d}J_2}{\mathrm{d}\xi} = 0$. Going back to (101), we have:

$$\frac{\mathrm{d}J_2}{\mathrm{d}\xi} = \frac{\alpha-1}{3\alpha^2}gB\left(\frac{\mathrm{d}B}{\mathrm{d}\xi} - \frac{\mathrm{d}}{\mathrm{d}\xi}\left(\frac{2h^{3/2}W}{m}\right)\right) - \frac{2}{3}\frac{\alpha-1}{\alpha^2}\frac{gh^{3/2}W}{m}\frac{\mathrm{d}B}{\mathrm{d}\xi}\,. \tag{104}$$

With (95), the term in brackets in the previous expression is nothing but $\dfrac{\mathrm{d}K}{\mathrm{d}\xi} = 0$. Going back to the definition $\theta(h) = \dfrac{gh^2}{m}\dfrac{\alpha-1}{\alpha}$ and using (100), wec thus get:

$$\frac{\mathrm{d}J_2}{\mathrm{d}\xi} = -\frac{4}{3}\frac{\theta W h}{\alpha m}\phi P - \left(\frac{4}{3}\frac{\theta^2W^2}{\alpha}\frac{h}{m}\phi + 2\frac{\theta W^2}{\alpha m}\right)\frac{\mathrm{d}h}{\mathrm{d}\xi} \tag{105}$$

Then, summing (103) and (105):

$$\mathcal{R} + \frac{\mathrm{d}J_2}{\mathrm{d}\xi} = \frac{4}{3}\frac{WP}{\alpha m}\left(\phi m - \frac{3}{2} - \phi h\theta\right) + \frac{4}{3}\frac{W^2\theta}{\alpha m}\left(\phi m - \phi h\theta - \frac{3}{2}\right)\frac{\mathrm{d}h}{\mathrm{d}\xi}\,.$$

But with (97), we have $\phi(m - h\theta) = \dfrac{3}{2}$, which immediately gives $\mathcal{R} + \dfrac{\mathrm{d}K_2}{\mathrm{d}\xi} = 0$. Eventually, returning to (102), we thus get:

$$\frac{\mathrm{d}J}{\mathrm{d}\xi} = \frac{\mathrm{d}J_1}{\mathrm{d}\xi} + \frac{\mathrm{d}J_2}{\mathrm{d}\xi} = -\frac{2a^2W}{m} + \left(g - \frac{m^2}{h^3} + \frac{P}{h} + \frac{a^2\alpha}{h}\right)\frac{\mathrm{d}h}{\mathrm{d}\xi}\,,$$

and consequently:

$$\frac{\mathrm{d}h}{\mathrm{d}\xi} = F(h,P,W) = \frac{2a^2W}{m}\left(g - \frac{m^2}{h^3} + \frac{P}{h} + \frac{a^2\alpha}{h}\right)^{-1}\,.$$

The equations for P and W directly follows from (99) and (98).

4.2 Proof of Proposition 4

This part is dedicated to the proof of the main results stated in Section §2.2. Before addressing these energy estimates, several notations and basic technical results are necessary.

4.2.1 Additional notations and duality results

In what follows we will regularly use the notation:

$$\mathcal{S}_K(a,b) = a_{K+1/2}b_{K+1/2} + a_{K-1/2}b_{K-1/2}\,, \tag{106}$$

with its natural generalization to the sum of interface products $\mathcal{S}_K(a_1,\cdots,a_n)$. When no confusion is possible, we will use the convention $\mathcal{S}_K(a^2) = \mathcal{S}_K(a,a)$. Remark that

$a_K\mathcal{S}_K(b) = \bar{a}_{K+1/2}b_{K+1/2} + \bar{a}_{K-1/2}b_{K-1/2} - [a]_{K+1/2}b_{K+1/2} + [a]_{K-1/2}b_{K-1/2}$, which gives the duality formula:

$$a_K\mathcal{S}_K(b) = \mathcal{S}_K(\bar{a}, b) - \Delta x \partial_K([a], b)\,. \tag{107}$$

Also, we have the following inequality:

$$\begin{aligned}\left[\partial_K(a,b)\right]^2 &= \frac{1}{\Delta x^2}\left(a_{K+1/2}b_{K+1/2} - a_{K-1/2}b_{K-1/2}\right)^2 \\ &\leqslant \frac{2}{\Delta x^2}\left(\left(a_{K+1/2}b_{K+1/2}\right)^2 + \left(a_{K-1/2}b_{K-1/2}\right)^2\right) = \frac{2}{\Delta x^2}\mathcal{S}_K(a^2, b^2)\,.\end{aligned} \tag{108}$$

Finally, introducing a third generic sequence of interface scalar quantities $(\mu_{K+1/2})_{K\in\mathbb{Z}}$, note that the discrete operators defined in (82), (57) and (58) are subject to the following elementary duality relations:

$$\widetilde{\partial_K^c}(a,b) = a_K\partial_K^c b + b_K\partial_K^c a\,, \tag{109}$$

$$a_K\partial_K\left(\mu, [b]\right) = b_K\partial_K\left(\mu, [a]\right) - \partial_K\left(\mu, [a], \bar{b}\right) + \partial_K\left(\mu, \bar{a}, [b]\right)\,. \tag{110}$$

$$a_K\partial_K\left(\mu, [a]\right) = \partial_K\left(\mu, \bar{a}, [a]\right) - \frac{1}{\Delta x}\mathcal{S}_K\left(\mu, [a]^2\right)\,. \tag{111}$$

4.2.2 Proof of Proposition 1

Since the water height does not evolve in time during this step, we will omit the subscript "n" when referring to the variable h in all the forthcoming developments. We first focus on the kinetic energy. Using the classical equality $(a-b)b = \frac{1}{2}a^2 - \frac{1}{2}b^2 - \frac{1}{2}(a-b)^2$, and the definition (68):

$$h_K\left(U_K^{n+1} - U_K^n\right)U_K^n = \mathcal{K}_K^{n+1} - \mathcal{K}_K^n - \frac{1}{2}h_K\left(U_K^{n+1} - U_K^n\right)^2\,.$$

Considering the discrete velocity equation (71), this leads to:

$$\mathcal{K}_K^{n+1} - \mathcal{K}_K^n = -\Delta t U_K^n\partial_K^c\left(hP^{n+1}\right) + \frac{1}{2}h_K\left(U_K^{n+1} - U_K^n\right)^2\,. \tag{112}$$

Similar relations are obtained for the energy associated with the other variables (see definitions (69)). Proceeding the same way for the variable B, we immediately obtain:

$$\mathcal{B}_K^{n+1} - \mathcal{B}_K^n = \Delta t\beta B_K^n\partial_K^c\left(2h^{3/2}W^{n+1}\right) + \frac{\beta}{2}h_K\left(B_K^{n+1} - B_K^n\right)^2\,. \tag{113}$$

On the other hand, we can write:

$$\frac{4}{3\alpha}h_K\left(W_K^{n+1} - W_K^n\right)W_K^{n+1} = \mathcal{W}_K^{n+1} - \mathcal{W}_K^n + \frac{2}{3\alpha}h_K\left(W_K^{n+1} - W_K^n\right)^2\,,$$

which leads to (we refer to (75) and (74) for the definitions of ξ_K^n and ζ_K^n and recall that $\beta = g\frac{\alpha-1}{3\alpha^2}$):

$$\begin{aligned}\mathcal{W}_K^{n+1} - \mathcal{W}_K^n &= \frac{4}{3\alpha}h_K W_K^{n+1}\left(\Delta t\frac{3}{2}\frac{P_K^{n+1}}{h_K} + \Delta t\frac{\alpha-1}{2\alpha}g\sqrt{h_K}\partial_K B^*\right) - \frac{2h_K}{3\alpha}\left(W_K^{n+1} - W_K^n\right)^2 \\ &= \frac{2\Delta t}{\alpha}(WP)_K^{n+1} + \beta\Delta t\left(2h_K^{3/2}W_K^{n+1}\right)\partial_K B^* - \frac{2h_K}{3\alpha}\Delta t^2\zeta_K^2\,.\end{aligned} \tag{114}$$

Doing the same for the variable P:

$$\frac{1}{\alpha a^2} h_K \left(P_K^{n+1} - P_K^n\right) P_K^{n+1} = \mathcal{P}_K^{n+1} - \mathcal{P}_K^n + \frac{1}{2\alpha a^2} h_K \left(P_K^{n+1} - P_K^n\right)^2 ,$$

which leads to:

$$\begin{aligned} \mathcal{P}_K^{n+1} - \mathcal{P}_K^n &= \frac{h_K}{\alpha a^2} P_K^{n+1} \left(-\Delta t a^2 \left[2 \frac{W_K^{n+1}}{h_K^n} + \alpha \partial_K U^* \right] \right) - \frac{h_K}{2\alpha a^2} \left(P_K^{n+1} - P_K^n\right)^2 \\ &= -\frac{2\Delta t}{\alpha} (WP)_K^{n+1} - \Delta t (hP)_K^{n+1} \partial_K U^* - \Delta t^2 \frac{a^2 h_K}{2\alpha} \xi_K^2 . \end{aligned} \tag{115}$$

Having in mind notations (78), we obtain, summing (112), (113), (114) and (115):

$$E_K^{n+1} - E_K^n = \mathcal{H}_K + \mathcal{G}_K , \tag{116}$$

where

$$\mathcal{H}_K = -\Delta t \left(U_K^n \partial_K^c R^{n+1} + R_K^{n+1} \partial_K U^* \right) + \frac{1}{2} h_K \left(U_K^{n+1} - U_K^n\right)^2 - \Delta t^2 \frac{a^2 h_K}{2\alpha} \xi_K^2 , \tag{117}$$

$$\mathcal{G}_K = -\Delta t \beta \left(B_K^n \partial_K^c S^{n+1} + S_K^{n+1} \partial_K B^* \right) + \frac{1}{2} \beta h_K \left(B_K^{n+1} - B_K^n\right)^2 - \Delta t^2 \frac{2 h_K}{3\alpha} \zeta_K^2 . \tag{118}$$

We focus now on the first part of the term (117). Going back to the definition (72) and the duality relation (109), we write:

$$\begin{aligned} U_K^n \partial_K^c R^{n+1} + R_K^{n+1} \partial_K U^* &= U_K^n \partial_K^c R^{n+1} + R_K^{n+1} \partial_K^c U - R_K^{n+1} \partial_K \Gamma \\ &= \widetilde{\partial_K^c} \left(U^n, R^{n+1}\right) - R_K^{n+1} \partial_K \Gamma . \end{aligned}$$

Following the same lines for the first term of (118), we also have:

$$B_K^n \partial_K^c S^{n+1} + S_K^{n+1} \partial_K B^* = \widetilde{\partial_K^c} \left(B^n, S^{n+1}\right) - S_K^{n+1} \partial_K \Theta ,$$

which allows to recover (79) with (80) and (81).

4.2.3 Proof of Proposition 2

This Proposition focuses on the first residual (80) appearing in (79). The following Lemma provides an estimate on the first contribution of this term:

Lemma 1. *Let $\lambda = \dfrac{\Delta t}{\Delta x}$. Assume that the stabilization term in (72) is of the form:*

$$\Gamma_{K+1/2} = \lambda c_g \mu_{K+1/2} [R^n]_{K+1/2} , \tag{119}$$

where $c_g > 0$ and $(\mu_{K+1/2})$ is a sequence of scalar interface values. Then, for any constant $\varrho > 0$, we have the following estimation:

$$\begin{aligned} \Delta t R_K^{n+1} \partial_K \Gamma \leqslant \Delta t \left(\mathcal{A}_K^1 + \mathcal{A}_K^2 \right) + \frac{1}{2} \Delta t^2 h_K \left(\frac{a^4 \lambda^2}{\varrho^2} \right) \xi_K^2 \\ + \lambda^2 c_g^2 \varrho^2 \mathcal{S}_K \left(\mu^2, \bar{h}, [R^{n+1}]^2 \right) - \lambda^2 c_g \mathcal{S}_K \left(\mu, [R^{n+1}]^2 \right) . \end{aligned} \tag{120}$$

The terms $\mathcal{A}_K^1$ and $\mathcal{A}_K^2$ are low-order antisymmetric contributions, respectively given by:

$$\mathcal{A}_K^1 = \lambda c_g \partial_K \left(\mu, \bar{R}^{n+1}, [R^n] \right) - \lambda c_g \partial_K \left(\mu, \bar{R}^n, [R^{n+1}] \right) , \tag{121}$$

$$\mathcal{A}_K^2 = -\lambda c_g^2 \varrho^2 \partial_K \left(\mu^2, [h], [R^{n+1}]^2 \right) + \lambda c_g \partial_K \left(\mu, \bar{R}^{n+1}, [R^{n+1}] \right) . \tag{122}$$

Proof. By direct application of formula (110), we write:

$$\begin{aligned}\Delta t R_K^{n+1}\partial_K\Gamma &= \lambda c_g \Delta t R_K^{n+1}\partial_K\left(\mu,[R^n]\right)\\ &= \lambda c_g \Delta t R_K^{n}\partial_K\left(\mu,[R^{n+1}]\right) + \Delta t\mathcal{A}_K^1\,.\end{aligned} \tag{123}$$

On the other hand:

$$\lambda c_g \Delta t R_K^{n}\partial_K\left(\mu,[R^{n+1}]\right) = -\lambda c_g\Delta t\left(R_K^{n+1}-R_K^n\right)\partial_K\left(\mu,[R^{n+1}]\right) + \lambda c_g\Delta t R_K^{n+1}\partial_K\left(\mu,[R^{n+1}]\right)\,. \tag{124}$$

With definition (78) and using the discrete evolution of P (77), the first term of the right hand side can be rewritten as:

$$-\lambda c_g\Delta t\left(R_K^{n+1}-R_K^n\right)\partial_K\left(\mu,[R^{n+1}]\right) = \lambda c_g\Delta t^2 a^2 h_K\xi_K\partial_K\left(\mu,[R^{n+1}]\right)\,, \tag{125}$$

and subject to the following estimation, with the help of inequality (108) and the duality formula (107):

$$\begin{aligned}\left|\lambda c_g\Delta t^2 a^2 h_K\xi_K\partial_K\left(\mu,[R^{n+1}]\right)\right| &= h_K\Delta t^2\left|\left(\frac{\lambda a^2\xi_K}{\varrho}\right)\left(c_g\varrho\partial_K\left(\mu,[R^{n+1}]\right)\right)\right|\\ &\leqslant \frac{1}{2}\Delta t^2 h_K\left(\frac{\lambda a^2\xi_K}{\varrho}\right)^2 + \frac{1}{2}\Delta t^2 h_K\left(c_g\varrho\partial_K\left(\mu,[R^{n+1}]\right)\right)^2\\ &\leqslant \frac{1}{2}\Delta t^2 h_K\left(\frac{\lambda^2 a^4}{\varrho^2}\right)\xi_K^2 + \lambda^2 c_g^2\varrho^2 h_K\mathcal{S}_K\left(\mu^2,[R^{n+1}]^2\right)\\ &\leqslant \frac{1}{2}\Delta t^2 h_K\left(\frac{\lambda^2 a^4}{\varrho^2}\right)\xi_K^2 + \lambda^2 c_g^2\varrho^2\mathcal{S}_K\left(\mu^2,\bar{h},[R^{n+1}]^2\right)\\ &\qquad - \Delta x\lambda^2 c_g^2\varrho^2\partial_K\left(\mu^2,[h],[R^{n+1}]^2\right)\,.\end{aligned} \tag{126}$$

With (111), the second term of the right hand side in (124) can be written as:

$$\lambda c_g\Delta t R_K^{n+1}\partial_K\left(\mu,[R^{n+1}]\right) = \lambda c_g\Delta t\partial_K\left(\mu,\bar{R}^{n+1},[R^{n+1}]\right) - \lambda^2 c_g\mathcal{S}_K\left(\mu,[R^{n+1}]^2\right)\,. \tag{127}$$

Summing estimations (126) and (127) and going back to (123), we get:

$$\begin{aligned}\Delta t R_K^{n+1}\partial_K\Gamma \leqslant\ & \Delta t\Big(\mathcal{A}_K^1 - \lambda c_g^2\varrho^2\partial_K\left(\mu^2,[h],[R^{n+1}]^2\right) + \lambda c_g\partial_K\left(\mu,\bar{R}^{n+1},[R^{n+1}]\right)\Big)\\ &+ \frac{1}{2}\Delta t^2 h_K\left(\frac{\lambda^2 a^4}{\varrho^2}\right)\xi_K^2 + \lambda^2 c_g^2\varrho^2\mathcal{S}_K\left(\mu^2,\bar{h},[R^{n+1}]^2\right) - \lambda^2 c_g\mathcal{S}_K\left(\mu,[R^{n+1}]^2\right)\,,\end{aligned}$$

which is nothing but (120). □

Based on this first result, we can now provide the following estimation:

Lemma 2. *Under the hypothesis of Lemma 1, the term $\mathbb{H}_K$ defined in (80) satisfies the following bound:*

$$\mathbb{H}_K \leqslant \Delta t\mathcal{A}_K + \lambda^2\mathbb{R}_K + \frac{1}{2\alpha}\Delta t^2\xi_K^2 a^2 h_K\left(\frac{\alpha a^2\lambda^2}{\varrho^2}-1\right)\,, \tag{128}$$

where

$$\mathbb{R}_K = c_g^2 \varrho^2 \mathcal{S}_K\left(\mu^2, \bar{h}, [R^{n+1}]^2\right) - c_g \mathcal{S}_K\left(\mu, [R^{n+1}]^2\right) + \mathcal{S}_K\left(\overline{1/h}, [R^{n+1}]^2\right) . \tag{129}$$

The contribution $\mathcal{A}_K$ stands for a residual flux term, defined as:

$$\mathcal{A}_K = \mathcal{A}_K^1 + \mathcal{A}_K^2 + \mathcal{A}_K^3 \tag{130}$$

with $\mathcal{A}_K^1$, $\mathcal{A}_K^2$ respectively given by (121), (122) and

$$\mathcal{A}_K^3 = -\lambda \partial_K\left([1/h], [R^{n+1}]^2\right) . \tag{131}$$

Proof. We recall that:

$$\mathbb{H}_K = \Delta t R_K^{n+1} \partial_K \Gamma + \frac{1}{2} h_K \left(U_K^{n+1} - U_K^n\right)^2 - \Delta t^2 \frac{a^2}{2\alpha} h_K \xi_K^2 . \tag{132}$$

We have, with (108) :

$$\frac{1}{2} h_K \left(U_K^{n+1} - U_K^n\right)^2 = \frac{1}{2} h_K \left(\frac{\Delta t}{h_K} \partial_K^c R^{n+1}\right)^2 \leqslant \frac{\lambda^2}{h_K} \mathcal{S}_K\left([R^{n+1}]^2\right) ,$$

and equality (107) allows to write:

$$\frac{1}{2} h_K \left(U_K^{n+1} - U_K^n\right)^2 \leqslant \lambda^2 \mathcal{S}_K\left(\overline{1/h}, [R^{n+1}]^2\right) - \lambda^2 \Delta x \partial_K\left([1/h], [R^{n+1}]^2\right) .$$

Using this inequality, together with the estimation (120) in (132):

$$\begin{aligned}
\mathbb{H}_K \leqslant\ & \Delta t \left(\mathcal{A}_K^1 + \mathcal{A}_K^2 - \lambda \partial_K\left([1/h], [R^{n+1}]^2\right)\right) \\
& + \frac{1}{2} \Delta t^2 h_K \left(\frac{a^4 \lambda^2}{\varrho^2}\right) \xi_K^2 - \Delta t^2 \frac{a^2}{2\alpha} h_K \xi_K^2 \\
& + \lambda^2 c_g^2 \varrho^2 \mathcal{S}_K\left(\mu^2, \bar{h}, [R^{n+1}]^2\right) - \lambda^2 c_g \mathcal{S}_K\left(\mu, [R^{n+1}]^2\right) + \lambda^2 \mathcal{S}_K\left(\overline{1/h}, [R^{n+1}]^2\right) ,
\end{aligned}$$

which gives the announced result. □

If we now assume that the stabilization term $\Gamma_{K+1/2}$ implied in (72) is given by (83) as in Proposition 2, we are in the frame of Lemma 1 with $\mu_{K+1/2} = \left(\overline{1/h}\right)_{K+1/2}$ and the estimate (128) stands. Setting $\varrho = a\lambda\sqrt{\alpha}$, the last term of the right hand side in (128) is zero and we are consequently left with the negativity of the residual (129). Considering the definition of $\mathcal{S}_K$ (106), the term $\mathbb{R}_K$ may be written as the sum of two interface contributions: $\mathbb{R}_K = \mathfrak{r}_{K+1/2} + \mathfrak{r}_{K-1/2}$ with

$$\mathfrak{r}_{K+1/2} = [R^{n+1}]^2 \left(\overline{1/h}\right)_{K+1/2} \left[c_g^2 \varrho^2 \left(\overline{1/h}\right)_{K+1/2} \overline{h}_{K+1/2} - c_g + 1\right] ,$$

wich leads to identify conditions ensuring $\mathfrak{r}_{K+1/2} \leqslant 0$ at the level of each cell interface. We thus have to ensure the negativity of the polynomial $p(c_g) = c_g^2 \varrho^2 \tau_{K+1/2} - c_g + 1$ (we recall that $\tau_{K+1/2} = \left(\overline{1/h}\right)_{K+1/2} \overline{h}_{K+1/2}$) which can be rewritten, according to $\varrho = a\lambda\sqrt{\alpha}$ and noting $\vartheta = 4a^2\lambda^2\alpha\tau_{K+1/2}$:

$$p(c_g) = c_g^2 \vartheta/4 - c_g + 1 . \tag{133}$$

The conditions for p to be negative immediately lead to (84) and (85). Therefore Lemma 2 gives $\mathbb{H}_K \leqslant \Delta t \mathcal{A}_K$, which concludes the proof of Proposition 2.

4.2.4 Proof of Proposition 3

The structure of the evolution equations of U and B (71) are similar, as well as the nature of the residuals (117) and (118). As a result the proof of Proposition 3 follows the same lines as previously. We just mention here the two Lemmas without detailing their proofs and discuss the conditions leading to the main result stated in Proposition 3.

Lemma 3. *Assume that the stabilization term in (73) is of the form:*

$$\Theta_{K+1/2} = c_t \lambda \mu_{K+1/2} [S^n]_{K+1/2} \,, \tag{134}$$

where $c_g > 0$ and $(\mu_{K+1/2})$ is a sequence of scalar interface value. Then, for any sequence of strictly positive scalars $(\varrho_K)_{K\in\mathbb{Z}}$, we have the following estimation:

$$\begin{aligned} \Delta t S_K^{n+1} \partial_K \Theta \leqslant \Delta t \left(\mathcal{B}_K^1 + \mathcal{B}_K^2 \right) + 2\Delta t^2 h_K^2 \left(\frac{\lambda^2}{\varrho_K^2} \right) \zeta_K^2 \\ + \lambda^2 c_t^2 \mathcal{S}_K \left(\mu^2, \overline{\varrho^2 h}, [S^{n+1}]^2 \right) - \lambda^2 c_t \mathcal{S}_K \left(\mu, [S^{n+1}]^2 \right) \,. \end{aligned} \tag{135}$$

The terms $\mathcal{B}_K^1$ and $\mathcal{B}_K^2$ are low order antisymmetric contributions, respectively given by:

$$\mathcal{B}_K^1 = \lambda c_t \partial_K \left(\mu, \bar{S}^{n+1}, [S^n] \right) - \lambda c_t \partial_K \left(\mu, \bar{S}^n, [S^{n+1}] \right) \,, \tag{136}$$

$$\mathcal{B}_K^2 = -\lambda c_t^2 \partial_K \left(\mu^2, [\varrho^2 h], [S^{n+1}]^2 \right) + \lambda c_t \partial_K \left(\mu, \bar{S}^{n+1}, [S^{n+1}] \right) \,. \tag{137}$$

Lemma 4. *Under the hypothesis of Lemma 3, the term $\mathbb{G}_K$ defined in (81) satisfies the following bound:*

$$\mathbb{G}_K^n \leqslant \Delta t \beta \mathcal{B}_K + \lambda^2 \beta \mathbb{P}_K + \Delta t^2 \frac{2h_K}{3\alpha} \zeta_K^2 \left(\lambda^2 \frac{g h_K (\alpha - 1)}{\alpha \varrho_K^2} - 1 \right) \,, \tag{138}$$

where

$$\mathbb{P}_K = c_t^2 \mathcal{S}_K \left(\mu^2, \overline{\varrho^2 h}, [S^{n+1}]^2 \right) - c_t \mathcal{S}_K \left(\mu, [S^{n+1}]^2 \right) + \mathcal{S}_K \left(\overline{1/h}, [S^{n+1}]^2 \right) \,. \tag{139}$$

The residual flux term $\mathcal{B}_K$ is defined as:

$$\mathcal{B}_K = \mathcal{B}_K^1 + \mathcal{B}_K^2 + \mathcal{B}_K^3 \tag{140}$$

with $\mathcal{B}_K^1$, $\mathcal{B}_K^2$ respectively given by (136), (137) and

$$\mathcal{B}_K^3 = -\lambda \partial_K \left([1/h], [S^{n+1}]^2 \right) \,. \tag{141}$$

Again, assuming (87), we are in the frame of Lemma 3 with $\mu_{K+1/2} = \left(\overline{1/h} \right)_{K+1/2}$, so that the estimate (138) is valid. Note that if $\beta = 0$ (that is $\alpha = 1$) the term is $\mathbb{G}_K$ is negative and does not need to be controlled. Otherwise, setting $\varrho_K = \lambda \sigma_K = \lambda \sqrt{g h_K \left(\dfrac{\alpha - 1}{\alpha} \right)} > 0$, the last term of the right hand side in (138) is zero and we have to ensure negativity of the residual (139). Considering the definition of $\mathcal{S}_K$ (106), the term $\mathbb{P}_K$ can be written as: $\mathbb{P}_K = \mathfrak{p}_{K+1/2} + \mathfrak{p}_{K-1/2}$ with

$$\mathfrak{p}_{K+1/2} = [S^{n+1}]^2 \left(\overline{1/h} \right)_{K+1/2} \left[c_t^2 \left(\overline{1/h} \right)_{K+1/2} \left(\overline{\varrho^2 h} \right)_{K+1/2} - c_t + 1 \right] .$$

Remarking that $\left(\overline{\varrho^2 h} \right)_{K+1/2} \leqslant \overline{h}_{K+1/2} \,.\, \max(\varrho_K^2, \varrho_{K+1}^2) = \lambda^2 \overline{h}_{K+1/2} \sigma_{K+1/2}^2$ where $\sigma_{K+1/2} = \max(\sigma_K, \sigma_{K+1})$, it is sufficient to ensure the negativity of the polynomial $p(c_t) = c_t^2 \lambda^2 \sigma_{K+1/2}^2 \tau_{K+1/2} - c_t + 1$, which gives sufficient conditions (88) and (89).

References

[1] S. Beji, J. Battjes. Experimental investigation of wave propagation over a bar. *Coast. Eng.*, **80**, 151–162, 1993.

[2] C. Berthon, A. Duran, F. Foucher, K. Saleh, J.D.D. Zabsonré. Improvement of the Hydrostatic Reconstruction Scheme to Get Fully Discrete Entropy Inequalities. *J. Sci. Comput.*, **80**, 924 – 956, 2019.

[3] J.L.. Bona, M. Chen, J.C. Saut. Boussinesq equations and other systems for small-amplitude long waves in nonlinear dispersive media. i: derivation and linear theory. *J. Nonlinear Sci.*, **12**, 283 – 318, 2002.

[4] P. Bonneton, F. Chazel, D. Lannes, F. Marche, M. Tissier. A splitting approach for the fully nonlinear and weakly dispersive Green-Naghdi model. *J. Comput. Phys.*, **230**, 1479–1498, 2011.

[5] J. Boussinesq. Théorie des ondes et des remous qui se propagent le long d'un canal rectangulaire horizontal, en communiquant au liquide contenu dans ce canal des vitesses sensiblement pareilles de la surface au fond. *J. mathématiques pures et appliquées*, 55–108, 1872.

[6] S. Busto, M. Dumbser, C. Escalante, N. Favrie, S. Gavrilyuk. On High Order ADER Discontinuous Galerkin Schemes for First Order Hyperbolic Reformulations of Nonlinear Dispersive Systems. *J Sci. Comput.* **87**(48), 2021).

[7] J.S.A. Do Carmo, J.A. Ferreira, L. Pinto, G. Romanazzi. An improved Serre model: Efficient simulation and comparative evaluation. *Applied Mathematical Modelling*, **56**, 404–423, 2018.

[8] F. Chazel, D. Lannes, F. Marche. Numerical Simulation of Strongly Nonlinear and Dispersive Waves Using a Green–Naghdi Model. *J. Sci. Comput.*, **48**, 105–116, 2011.

[9] D. Clamond, D. Dutykh, D. Mitsotakis. Conservative modified Serre–Green–Naghdi equations with improved dispersion characteristics. *Communications in Nonlinear Science and Numerical Simulation*, **45**, 245–257, 2017.

[10] F. Couderc, A. Duran, J.P. Vila. An explicit asymptotic preserving low Froude scheme for the multilayer shallow water model with density stratification. *Journal of Computational Physics*, **343**, 235–270, 2017.

[11] J.W. Daily, S.C. Stephan. Rigorous justification of the Favrie–Gavrilyuk approximation to the Serre–Green–Naghdi model. *Coastal Engineering Proceedings*, **1(3)**, 2, 1952.

[12] A. Del Grosso, M.J. Castro, A. Chan, G. Gallice, R. Loubère, P.-H. Maire. A well-balanced, positive, entropy-stable, and multi-dimensional-aware finite volume scheme for 2D shallow-water equations with unstructured grids, *Journal of Computational Physics*, **503**, 2024..

[13] H. Dong, M. Li. A reconstructed central discontinuous Galerkin-finite element method for the fully nonlinear weakly dispersive Green–Naghdi model. *Applied Numerical Mathematics*, **110**, 110–127, 2016.

[14] V. Duchêne. Rigorous justification of the Favrie–Gavrilyuk approximation to the Serre–Green–Naghdi model. *Nonlinearity*, **32**, 3772, 2019.

[15] V. Duchêne. Many Models for Water Waves. *HDR, Université de Rennes 1*, 2021.

[16] A. Duran, F. Marche. Discontinuous Galerkin discretization of Green-Naghdi equations on unstructured simplicial meshes. *Applied Mathematical Modelling* , **45**, 840–864, 2017.

[17] A. Duran, G. L. Richard. Modelling coastal wave trains and wave breaking. *Ocean Model.*, **147**, 101581, 2020.

[18] A. Duran. Revisiting energy estimates of the CPR scheme for the Shallow Water equations. *Submitted, hal preprint available at https://hal.science/hal-04220336*, 2023.

[19] L. Emerald. Rigorous Derivation from the Water Waves Equations of Some Full Dispersion Shallow Water Models. *SIAM Journal on Mathematical Analysis.*, **53**, 3772–3800, 2021.

[20] C. Escalante, M. Dumbser, M. Castro. An effcient hyperbolic relaxation system for dispersive non-hydrostatic water waves and its solution with high order discontinuous galerkin schemes, *J. Comput. Phys.*, **394**, 385–419, 2019.

[21] C. Escalante, T. Morales de Luna. A general non-hydrostatic hyperbolic formulation for Boussinesq dispersive shallow flows and its numerical approximation, *J. Sci. Phys.*, **83**(3), 1–37, 2020.

[22] C. Escalante, E.D. Fernández-Nieto, J. Garres-Díaz, T. Morales de Luna, Y. Penel. Non-hydrostatic layer-averaged approximation of Euler system with enhanced dispersion properties. *Computational and Applied Mathematics*, **42**(177), 2023.

[23] N. Favrie, S. Gavrilyuk. A rapid numerical method for solving Serre–Green–Naghdi equations describing long free surface gravity waves. *Nonlinearity*, **30**(7), 2718–2736, 2017.

[24] J.L. Guermond, B. Popov, E. Tovar, C. Kees. Robust explicit relaxation technique for solving the Green-Naghdi equations *Journal of Computational Physics*, **399**, 108917, 2019.

[25] J.L. Guermond, C. Kees, B. Popov, E. Tovar. Hyperbolic relaxation technique for solving the dispersive Serre–Green–Naghdi equations with topography *Journal of Computational Physics*, **450**, 110809, 2022.

[26] E.D. Fernández-Nieto, M. Parisot, Y. Penel, J. Sainte-Marie. A hierarchy of dispersive layer-averaged approximations of Euler equations for free surface flows. *Commun. Math. Sci.*, **16**(5), 1169-–1202, 2018.

[27] A. Green, P. Naghdi. A derivation of equations for wave propagation in water of variable depth. *J. Fluid Mech.*, **78**(2), 237-246, 1976.

[28] S. Gavrilyuk, K.-M. Shyue. 2D Serre-Green-Naghdi Equations over Topography: Elliptic Operator Inversion Method. *J. Fluid Mech.*, **150**(1), 237-246, 2023.

[29] A. Duran, G. L. Richard. A new model of shoaling and breaking waves: one-dimensional solitary wave on a mild sloping beach. *J. Fluid Mech.*, **862**, 552–591, 2019.

[30] M. Kazolea, M. Ricchiuto. On wave breaking for Boussinesq-type models. *Ocean Modelling*, **123**, 16–39, 2018.

[31] M. Kazolea, A.G. Filippini, M. Ricchiuto. Low dispersion finite volume/element discretization of the enhanced Green–Naghdi equations for wave propagation, breaking and runup on unstructured meshes. *Ocean Modelling*, **182**, 102157, 2023.

[32] S. Kivva. Entropy Stable Flux Correction for Hydrostatic Reconstruction Scheme for Shallow Water Flows. *Journal of Scientific Computing*, **99**, 2024.

[33] D. Lannes. The water waves problem: mathematical analysis and asymptotics. *American Mathematical Soc.*, **188**, 2013.

[34] D. Lannes, F. Marche. A new class of fully nonlinear and weakly dispersive green-naghdi models for efficient 2d simulations. *J. Comput. Phys.*, **282**, 238–268, 2015.

[35] Z. Liu, Z. Sun. Two sets of higher-order Boussinesq-type equations for water waves. *Ocean Eng.*, **32**, 1296–1310, 2005.

[36] Z. Liu, K. Fang, Y. Cheng. A new multi-layer irrotational boussinesq-type model for highly nonlinear and dispersive surface waves over a mildly sloping seabed. *J. Fluid Mech.*, **842**, 323–353, 2018.

[37] M. Li, L. Xu, Y. Cheng. A CDG-FE method for the two-dimensional Green-Naghdi model with the enhanced dispersive property. *J. Comput. Phys.*, **399**, 2019.

[38] R. Lteif. An operator-splitting approach with a hybrid finite volume/finite difference scheme for extended Boussinesq models. *Applied Numerical Mathematics*, **196**, 159–182, 2024.

[39] P.A. Madsen, O.R.. Sørensen. A new form of the boussinesq equations with improved linear dispersion characteristics. part 2. A slowly-varying bathymetry *Coastal Engineering*, **18**(3,4), 183–204, 1992.

[40] P.A. Madsen, B. Banijamali, H.A. Schäffer, O.R. Sørensen. Boussinesq type equations with high accuracy in dispersion and nonlinearity. *Coastal Engineering*, 95–108, 1996.

[41] P.A. Madsen, H.B.. Bingham, H. Liu. A new boussinesq method for fully nonlinear waves from shallow to deep water. *J Fluid Mech.*, **462**, 1–30, 2002.

[42] F. Marche. A combined Hybridized Discontinuous Galerkin (HDG) and Discontinuous Galerkin (DG) discrete formulation for Green-Naghdi equations on unstructured meshes. *J. Comput. Phys.* , **418**, 109637, 2020.

[43] O. Le Métayer, S. Gavrilyuk, S. Hank. A numerical scheme for the Green–Naghdi model. *Journal of Computational Physics* , **229**, 2034–2045, 2010.

[44] D. Mitsotakis, B. Ilan, D. Dutykh. On the Galerkin/Finite-Element Method for the Serre Equations. *J. Sci. Comput.* , **61**, 166–195, 2014.

[45] S. Noelle, M. Parisot, T. Tscherpel. A class of boundary conditions for time-discrete Green-Naghdi equations with bathymetry. *SIAM Journal on Numerical Analysis*, 2022.

[46] O. Nwogu. Alternative form of boussinesq equations for nearshore wave propagation. *Journal of waterway, port, coastal, and ocean engineering*, **119**(6), 618–638, 1993.

[47] N. Panda, C. Dawson, Y. Zhang, A.B. Kennedy, J.J. Westerink, A.S. Donahue. Discontinuous Galerkin methods for solving Boussinesq–Green–Naghdi equations in resolving non-linear and dispersive surface water waves. *Journal of Computational Physics*, **273**, 572 – 588, 2014.

[48] M. Parisot and J.P. Vila. Centered-potential regularization of advection upstream splitting method : Application to the multilayer shallow water model in the low Froude number regime. *SIAM Journal on Numerical Analysis*, **54**, 3083 – 3104, 2016.

[49] D.H. Peregrine. Long waves on a beach. *J. Fluid Mech.*, 815–827, 1967.

[50] J.P.A. Pitt, C. Zoppou, S.G. Roberts. Numerical scheme for the generalised Serre–Green–Naghdi model. *Wave Motion*, **115**, 2022.

[51] S. Popinet. A quadtree-adaptive multigrid solver for the Serre–Green–Naghdi equations. *Journal of Computational Physics*, **302**, 336–358, 2015.

[52] G.L. Richard. An extension of the Boussinesq-type models to weakly compressible flows. *European Journal of Mechanics - B/Fluids*, **89** 217–240, 2021.

[53] M. Rigal, C. El Hassanieh, J. Sainte-Marie. Implicit kinetic schemes for the Saint-Venant system. *preprint hal-04048832*, 2023.

[54] A. Samii, C. Dawson. An explicit hybridized discontinuous Galerkin method for Serre–Green–Naghdi wave model. *Computer Methods in Applied Mechanics and Engineering*, **330** 447–470, 2018.

[55] F. Serre. Contribution à l'étude des écoulements permanents et variables dans les canaux. *La Houille Blanche*, **6** 830–872, 1953.

[56] S. Tkachenko, S. Gavrilyuk, J. Massoni. Extended Lagrangian approach for the numerical study of multidimensional dispersive waves: Applications to the Serre-Green-Naghdi equations. *Journal of Computational Physics*, **477** 111901, 2023.

[57] M. Tonelli, M. Petti. Hybrid finite volume – finite difference scheme for 2DH improved Boussinesq equations. *Coastal Engineering*, **56**, 609–620, 2009.

[58] G. Wei, J.T. Kirby, S.T. Grilli, and R. Subramanya. A fully nonlinear Boussinesq model for surface waves. I. Highly nonlinear unsteady waves. *Journal of Fluid Mechanics*, **294**, 71–92, 1995.

[59] M. Zefzouf, F. Marche. A new symmetric interior penalty discontinuous Galerkin formulation for the Serre–Green–Naghdi equations. *Numer. Methods Partial Differ. Eq.*, **39**, 1478—1503, 2023.